MSc Research Thesis

Probabilisitic Seismic Hazard Assessment for the Southern part of the Netherlands

Denise de Vos (3037584)
Utrecht University, June 30, 2010

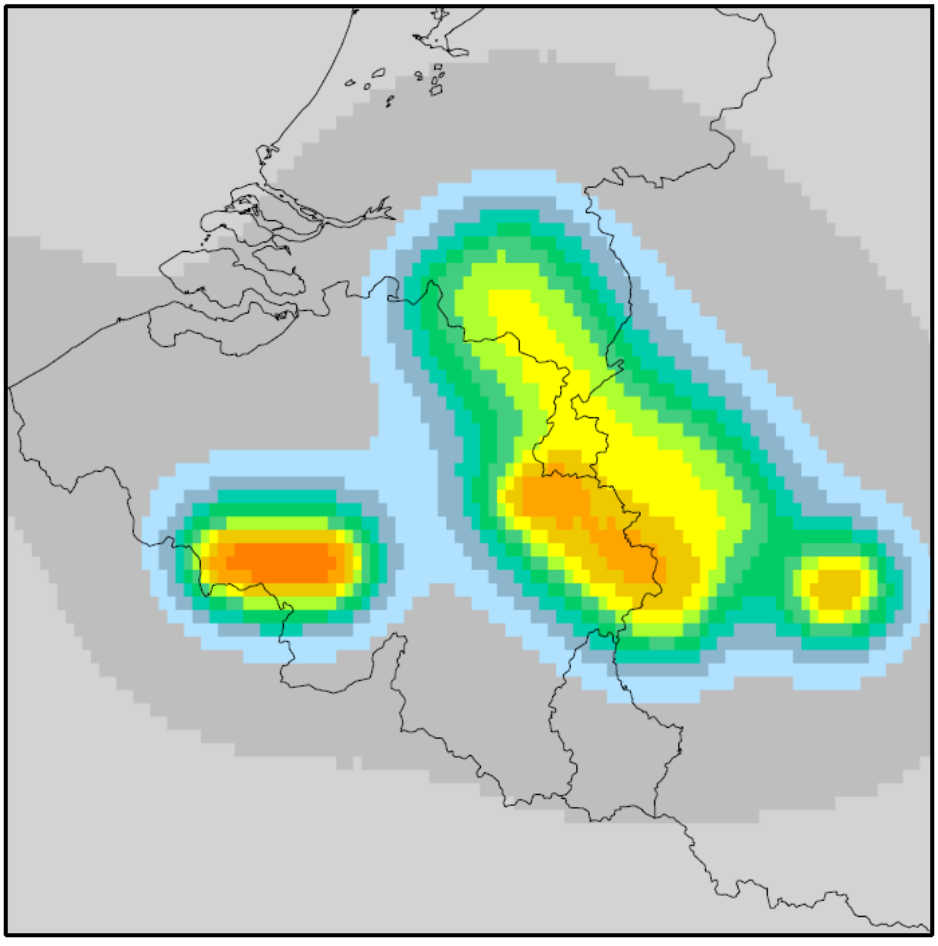

Supervisors:
Femke Goutbeek (KNMI) & Hanneke Paulssen (UU)

Abstract
Due to the necessity of a national Annex for the Eurocode 8, safety requirements of engineering structures and public interest in the effect of induced earthquakes, an update of the seismic hazard assessment is required for the Netherlands. A first version of a new seismic hazard model for tectonic seismicity is prepared, using two separate probabilistic seismic hazard methodologies. The input parameters (zonation, magnitude-frequency relation, ground motion prediction equation) are determined from the most recent earthquake catalogue and from the literature.

In the first method the analytical equations of the Probabilistic Seismic Hazard Analysis (PSHA) method of Cornell (1968) are numerically approached in the program EQRISK (McGuire, 1976). This method is developed for larger tectonic earthquakes, and turns out to be inappropriate to apply to low-seismicity areas, such as the Netherlands. An alternative approach of PSHA, based on a Monte Carlo simulation, is used in the new national Eurocode 8 Annex in the United Kingdom. The M3C hazard software presented by Musson (2009) is used to model the seismic hazard for the Netherlands.

Since little data are available for the Netherlands, the seismic hazard analysis admits to a wide range of interpretations and uncertainties. The sensitivity of the hazard estimate to the input parameters is investigated. It turns out that the hazard estimate is mainly sensitive to the definition of source zonation and the choice of ground motion prediction equation.

Finally, the revised seismic hazard map presented in this study is compared to alternative studies, which are performed for surrounding countries. The results of Leynaud et al. (2000) agree fairly well with those presented in this study. Probably due to the use of another zonation model, the seismic hazard maps of Meskouris (2005) and Grünthal et al. (2007) is more different, although in the Roer Valley region similar peak ground accelerations are expected. The results of this study are quite different from those of a former study (De Crook, 1996). This is probably due to the smaller amount of data used for the former study and the use of another source definition.

The final proposed seismic hazard map contains regions for which (taking the uncertainty into account) the critical value mentioned in the Eurocode 8 will most probably not be exceeded in 475 years. For the remaining areas (*i.e.* Roer Valley, Hainaut zone, the areas surrounding Liège and Hautes Fagnes and the Neuwied basin), the PGA values are just below, or above the critical value. It is up to the user to decide whether seismic hazard should be taken into account. For further research it is recommended to quantify the uncertainty of the hazard estimate.

Acknowledgements
Special thanks to Femke Goutbeek, for supervising this MSc Research, as well as to Torild van Eck and Bernard Dost. The conversations we had and their criticism were very valuable. Also, appreciation is extended to Hanneke Paulssen, for being the second supervisor and stimulating me to have a critical view on the results. R.M.W. Musson kindly provided the M3C program and gave valuable response to my questions, for which I am thankful. Several papers were provided by K. Campbell, K.-G. Hinzen, R.M.W. Musson and the Royal Observatory of Belgium. I am also grateful to Jasper Schuur, for his mental support and the useful suggestions for the oral presentation of this research. Finally, I would like to thank the entire team of KNMI, department of Seismology, for the great time I had during this research.

Contents

Introduction *2*
1 **Probabilistic Seismic Hazard Analysis *4***
1.1 *Theory 4*
1.2 *Methodologies 9*
1.2.1 Numerical approach of the analytical equations *10*
1.2.2 Monte Carlo approach *11*
2 **Input models *12***
2.1 *Source zones 12*
2.2 *Seismicity characterization 18*
2.3 *Ground Motion Prediction Equations 20*
2.4 *Local site effects 23*
2.5 *Uncertainties 23*
2.5.1 Ground motion prediction equation *24*
2.5.2 Focal depth *26*
2.5.3 Minimum magnitude *28*
2.5.4 Maximum magnitude *33*
2.5.5 Seismicity parameters *34*
2.5.6 Source zone definition *37*
3 **Results *41***
3.1 *Analytical approach 41*
3.2 *Monte Carlo approach 42*
4 **Discussion and Conclusions *45***
4.1 *Comparison to other seismic hazard models 45*
4.2 *Recommendations for the improvement of the model 51*
Appendix *53*
Bibliography *56*

Introduction

Seismic hazard is the likelyhood, or probability, of experiencing a specified intensity of any damaging phenomenon at a particular site, or in a region, in some period of interest (Thenhaus and Campbell, 2003). Seismic activity can have a natural cause, such as tectonic stresses in the crust. Also, stress changes as a consequence of human influences, such as gas exploration, can occur, which results in so-called induces earthquakes. Since, especially in regions of high seismicity and dense population, ground-shaking can cause large human and economic losses, seismic hazard analysis is an important issue.

Although seismic activity in the Netherlands is known to be low to moderate, some damaging earthquakes occurred in the past. Due to the safety requirements of engineering structures and public interest in the effect of induced earthquakes seismic hazard analysis has become more important in the Netherlands. On a European level, general guidelines for building codes with respect to earthquakes have been defined in Eurocode 8. These guidelines state that for the building of special engineering structures (such as nuclear power plants, gas storage tanks etcetera) seismic hazard has to be taken into account in areas where an exceedence of peak ground acceleration (PGA) is expected of 0.1 g (1 $g = 981\ cm/s^2$). Each European country has the opportunity to develop its own annex for the Eurocode, which describes how this code is applicable to the country. In contrast to Germany and Belgium, there is no such annex available yet for the Netherlands. In order to develop a national Annex for Eurocode 8, a seismic hazard map of the Netherlands is required, which shows where the hazard exceeds 0.1 g. Also, since engineering structures respond differently to different frequencies, there should be information about the dominant frequencies that are present in seismic waves that occur in the area. In areas where the limiting value of ground acceleration is expected to be exceeded for a return period of 475 yrs, engineers have to design their structures in such a way that they are resistant to the accelerations and frequencies that could be expected.

The latest seismic hazard study for tectonic seismicity (*i.e.* earthquakes with a natural cause) in the Netherlands (De Crook, 1993) was based on intensities. Intensity is an indirect and non-objective hazard parameter, since it is based on public observations. A conversion of this seismic hazard map to peak ground accelerations has been performed by De Crook (1996). In the last decade, however, the earthquake catalogue, as well as the ground motion prediction equations, have been improved and updated. Therefore, a revised seismic hazard map of the Netherlands is necessary. The aim of this study is to prepare a preliminary version of a new seismic hazard model for the Netherlands based on peak ground acceleration (PGA), which incorporated innovative approaches. For now, only natural earthquakes will be considered, but the model might be extended to induced seismicity in later studies.

Different (probabilistic) methods are available for seismic hazard studies. In

order to investigate the influence of different approaches, two separate probabilistic seismic hazard methodologies will be used to carry out seismic hazard assessment for the Netherlands.

Initially, a standard hazard map is estimated using the Probabilistic Seismic Hazard Analysis (PSHA) method of Cornell (1968). The analytical equations of this method are numerically approached in the program EQRISK, of which the first version was written by McGuire (1976). Since this method is developed for larger tectonic earthquakes, the question rises whether it is appropriate to apply this to areas with low and (sometimes) shallow seismicity, such as the Netherlands. An alternative approach to PSHA, based on a Monte Carlo simulation, has been proposed by Musson (1999) and is used in the new national Eurocode8 Annex in the United Kingdom (Musson and Sargeant, 2007). Both the M3C (version 3) hazard software presented by Musson (2009) and EQRISK are used to model the seismic hazard for the Netherlands. Both programs require approximately the same input parameters (zonation, magnitude-frequency relation, ground motion prediction equation), which are determined from the most recent earthquake catalogue and from the literature.

Subsequently, the variability of the seismic hazard will be determined and visualized. This means that the effect of varying input parameters such as seismicity (rate and b-value), attenuation (different relations) and seismic zonation to the estimated hazard is investigated.

After several runs are performed and the seismic hazard estimate has been tested for sensitivity, a decision will be made on what combination(s) of parameters is/are the most plausible. The resulting seismic hazard map should be the basis for the national annex for Eurocode 8.

The revised seismic hazard maps presented in this study will be compared to alternative studies, performed for other countries surrounding the Netherlands (Leynaud et al. (2000), Meskouris (2005),Grünthal et al. (2007)). Since these areas are all characterised by a low seismicity, earthquake catalogues tend to be rather small. As a consequence, determination of seismicity parameters is difficult and they usually go together with large uncertainties. Also, for the derivation of the ground motion prediction equations often additional data from other countries are used, or the uncertainty is very large.

Chapter 1

Probabilistic Seismic Hazard Analysis

Seismic hazard analysis is the estimation of the maximum amplitude of some ground motion parameter (*e.g.* peak ground acceleration, peak ground velocity, relative displacement, etc.) expected to occur once at a certain site or area within a particular time span. This time span is referred to as the return period, which is the reciprocal of the annual probability of occurrence of a certain amplitude (Thenhaus and Campbell, 2003). Seismic hazard is often displayed in a ground motion hazard map, which illustrates the regional differences in expected ground motion amplitude (typically PGA) at a constant return period.

Two different fundamental types of seismic hazard analysis exist; deterministic and probabilistic methods. In deterministic analyses the effect at a site of either a single or a small amount of earthquake scenarios is considered (Thenhaus and Campbell, 2003). This method is less complicated than probabilistic analysis, but it is difficult to define one representative earthquake. In contrast, probabilistic analysis allows the use of multi-valued or continuous events and models (Reiter, 1990). Using this method, hazard estimations incorporate the effects of all earthquakes that could affect the site in question. Thus, instead of defining one maximum earthquake, all earthquakes having a magnitude within a chosen range are taken into account. The frequency of occurrence gives the probability of each earthquake.

Although there are some faults present, seismicity in the Netherlands is scattered, rather than large amounts of events occur along a particular fault. It is therefore better to take all events within a certain region into account and integrate over this area, than chosing one representative earthquake. Although it is more complicated than deterministic methods, probabilistic seismic hazard analysis (PSHA) is used to estimate the seismic hazard in the Netherlands and therefore only this method will be described in detail.

1.1 Theory

Before going into detail to the probabilistic seismic hazard assessment, it is important to note that the input, which is based on statistical seismicity information, sources and attenuation, is always a model. The input model is partly based on assumptions, and so is the outcome. One should therefore keep in mind that output models are sensitive to the input parameters, of which some are more critical than others.

A simplified statistical model of seismicity occurrence frequently used in PSHA is the so-called Poisson model, which states that earthquakes have no 'mem-

ory'. This implies that each earthquake occurring would have no influence on the size, timing and location of any other earthquake. Although this is obviously not the case in reality – after all, fore-/and aftershocks are well-known phenomena –, inclusion of the assumption, at least when known fore-/and aftershocks are removed from the dataset, simplifies the PSHA significantly. More complex models exist, but often insufficient statistical data are available to adopt a non-Poissonian assumption (Cornell, 1968).

The methodology used in most probabilistic seismic hazard analyses was first defined by Cornell (1968). PSHA requires 4 steps (Reiter, 1990), which are shown in figure 1.2:

1. Determine sources (line or area sources) of uniform earthquake potential. This means that for line or area sources implicitly the assumption is made that the probability of an earthquake of a given size occurring is constant throughout the source. A seismotectonic zone is defined by its observed seismicity, its geophysical, geological and tectonic characteristics and its place within a larger tectonic framework (De Crook, 1993). Unlike deterministic methods, which only use the closest source-to-site distance, PSHA requires integration over the entire source zone resulting in a range of distances from all possible locations within the source, since earthquakes are assumed to occur anywhere within the source zone.
2. In contrast to picking one controlling earthquake in deterministic seismic hazard analysis, PSHA requires the specification of an earthquake probability distribution function or recurrence relationship for each source, which is in the simple case given by:

$$Log\ N = A - BM \tag{1.1}$$

representing a straight line, which can be found by taking the best fit through the data set of observations. Due to the limited amount of samples, usually a maximum likelyhood estimator is used. N is the cumulative annual number of earthquakes of a given magnitude or larger that are expected to occur, A is the logarithm of the number of earthquakes of magnitude zero or greater expected to occur during the same time and B characterizes the proportion of large to small earthquakes. M is the earthquake magnitude.
The recurrence relationship gives the probability that an earthquake of a certain magnitude occurs anywhere inside the source area during the specific period of time. It is very important to use a complete dataset, since otherwise an inappropriate recurrence relationship will be found. Not all low magnitude earthquakes are recorded and therefore it is useful to choose a lower bound magnitude; not considering magnitudes lower than the minimum magnitude is allowed, since small earthquakes are thought tp have no significant contribution to the hazard. However, the seismicity parameters (A and B) are estimated for these magnitudes. Furthermore, when a poissonian model is assumed, fore-and aftershocks should be removed from the dataset, as stated earlier.
Since earthquake magnitude depends on the size of the fault, there is a physical upper limit on magnitude for each zone. The maximum earthquake is defined as the strongest earthquake that is physically achievable within, or on, a defined seismic source. For line sources the fault rupture parameters (a.o. rupture length, area and displacement), and therefore the maximum

magnitude, can be estimated using empirical correlation equations. These are relations that describe the correlation between fault rupture parameters and earthquake size; many studies have been made regarding determination of such empirical relationships. Since for area source zones, which generally have a lack of recognizable faults and seismically active geologic structures, fault rupture parameters are barely known and the prospects of doing a reasonable maximum earthquake estimation are limited.
Maximum earthquake magnitudes for area sources are typically estimated from historical earthquake data, worldwide analogs of the regional tectonic setting, regional paleoseismic data and interpretations (if available), or from the judgments of experts (Thenhaus and Campbell, 2003). When historical data are used, it is generally assumed that the largest historical event is the minimum value for a maximum earthquake estimate. If plenty of historical data would be available, this would result in a proper estimation of the maximum earthquake. Unfortunately, the historical period of reporting is often very short and it is therefore likely that the maximum possible earthquake is larger than the maximum historical event, but has not occurred or been sampled yet. When data are implemented from other regions in the world with a tectonic setting similar to that of the site of interest, the reliability of the maximum earthquake estimation increases. Paleoseismic data, such as paleoliquefaction, extend the record of earthquakes into prehistoric time. Liquefaction mainly accompanies large earthquakes, so considerably larger magnitudes than the historical ones can be estimated from prehistoric data. Unfortunately, paleoseismic data frequently have a large error and low reliability. For example, paleoseismic studies have been performed for the Netherlands (Berg et al., 2002), but the results are very inaccurate and cannot be used for maximum magnitude estimation in this study.

3. In order to determine the seismic hazard at a certain location, the ground motion caused by an earthquake of specific magnitude needs to be estimated. For this purpose, many ground motion prediction equations (attenuation relations) have been developed. Usually such relations are empirically determined, based on data from different regions, and it is the analysts job to decide which curve is suitable for the region of interest.
For the development of such ground motion prediction equations, several statistical regression techniques are available. Strong motion data, recorded under different conditions, are brought together and allow to make an estimation of ground motion for many earthquake scenarios. Ground motion depends on source type (magnitude), travel path (geometrical spreading and attenuation), travel distance and local site conditions (see section 2.4). Ground motion regression equations are defined as (Campbell, 1985):

$$\hat{Y} = b_1 f_1(M) f_2(R) f_3(M,R) f_4(P_i) \sigma \tag{1.2}$$

where $\hat{Y}$ is the strong motion parameter to be estimated, b_1 a constant scaling factor, $f_1(M)$, $f_2(R)$, $f_3(M,R)$ are functions of the independent variables magnitude, source-to-site distance, or both, respectively. Inclusion of f_3 would imply that the relative change in ground motion as a result of changes in magnitude and distance are not independent of each other (Reiter, 1990). This results in an attenuation curve of which the shape is dependent on magnitude, so a curve of ground motion with respect to distance changes shape

when another fixed magnitude is used. $f_4(P_i)$ is a set of functions representing possible source, site or building effects and σ gives the uncertainty in $\hat{Y}$.
Because the distribution of $\hat{Y}$ is approximately lognormal and additive formulas are easier to deal with, equation (1.2) can be rewritten as:

$$\begin{aligned} ln\ \hat{Y} &= ln\ b_1 + ln\ f_1(M) + ln\ f_2(R) \\ &\quad + ln\ f_3(M,R) + ln\ f_4(P_i) + ln\ \sigma \end{aligned} \tag{1.3}$$

Datasets used for estimation of an attenuation relation can be very different, depending on the way of measuring and choices on how to select the data. Most often strong motion measurements are in terms of peak ground acceleration (PGA), but also peak ground velocity (PGV), peak ground displacement, response spectral ordinates and Fourier spectral ordinates are used.
From an engineering viewpoint, horizontal components are much more important than vertical components, since usually most damage is caused by horizontal ground motion. Most studies therefore only consider the two perpendicular horizontal components. These separate components can be treated in different ways (Campbell, 1985); for example, the mean of the two horizontal components can be used, or the largest component. This results in relative over-/and underestimations of ground motion.
Also, magnitude can be defined in several different ways. In some studies moment magnitude (M_W) is preferred, whereas others use surface wave (M_S) or local magnitude (M_L). Usually, the magnitude scale in which most data are given is used. Relations between separate scales do exist, but conversion of data to other scales is often avoided, because it increases the uncertainty of hazard estimation. Attenuation relations are usually made for a specific kind of magnitude; this determines what magnitude type is required.
Another important parameter is source-to-site distance. Again, this variable can be defined in different ways, which is shown in figure 1.1. Distance measures most commonly used are distance from the earthquake fault rupture or epicentral or hypocentral distance. The latter are more appropriate for area sources, since often no fault planes are specified and small earthquakes can be treated as point sources instead of fault planes. For large source-to-site distances the difference between these definitions is very small, but when the site is close to the earthquake location the choice of distance measure is very important. Therefore, when using a derived attenuation relation, there needs to be consistency in distance measure.
The standard deviation of an attenuation relationship can be quite large (Campbell, 1985). Campbell (1997) states that the standard deviation of a ground motion estimation relation can be significantly reduced by separation of the strong motion database according to fault-rupture style (fault mechanism).
Besides factors such as magnitude and distance, the amplitude of the ground motion also depends on the properties of the material through which waves propagate. Different site classes amplify motions in a different way. These site effects mainly occur on a local scale, close to the receiver (*i.e.* in the upper

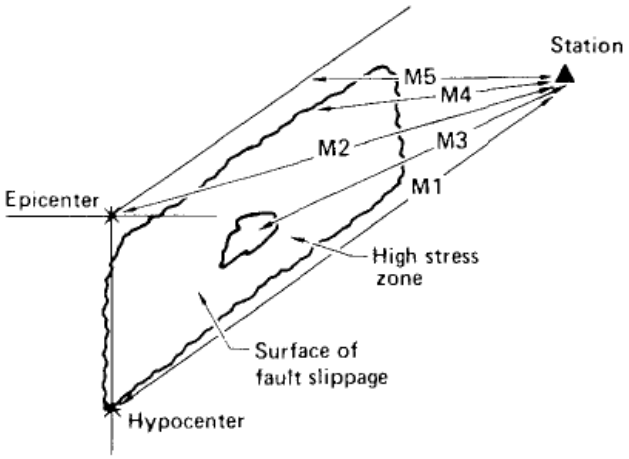

Figure 1.1: Schematic illustration of methods of source-to-site distance measurement. M1 = hypocentral distance (d_h); M2 = epicentral distance (d_e); M3 = distance to energetic zone; M4 = distance to slipped fault; M5 = distance to surface projection of fault (d_f) (after Shakal and Bernreuter (1981)).

$30 - 100\ m$). The properties which most affect the level of ground motion are impedance (*i.e.* resistance to particle motion) and absorption (Reiter, 1990). Sites consisting of low density and low velocity soil will experience higher amplitudes due to a certain earthquake than sites at the same distance consisting of high density and high velocity rock, because the impedance contrast in the latter site is higher. Absorption, in contrast, tends to be greater on soft soil than on hard rock (Reiter, 1990). It is therefore often useful to make a distinction in site classes occurring in the region of interest. Site classes are usually defined in broad categories, such as rock, soft rock, firm soil, soft soil, or they are defined by soil shear wave velocities.

The ground motion amplitude is also affected by the configuration of the underlying material. Sharp changes in rock properties cause reflections and conversion to other wave types, resulting in a change in amplitude. Also, resonance can occur, due to reverberation of waves being trapped in a layer. Furthermore, when upgoing and downgoing SH-waves being reflected at the surface are in phase, the free surface effect occurs, which means that the surface displacement is doubled.

Usually, layers are assumed to be horizontal, since lateral inhomogeneity would introduce additional complications. However, in some regions, for example in sediment-filled basins, this is not a good approximation and amplitudes could be seriously underestimated.

4. Finally, the effects of all earthquakes of different sizes, locations, sources and probabilities of occurrence are combined into one seismic hazard estimate. This is given by:

$$E(z) = \sum_{i=1}^{N} \alpha_i \int_{m_0}^{m_u} \int_{r=0}^{r=\infty} f_i(m) g_i(r) P(Z > z|m, r) dr dm \tag{1.4}$$

$E(z)$ is the expected number of exceedances of ground motion level z during

a specific time period. Due to the summation over i all sources are taken into account. α_i is the mean rate of occurrence of earthquakes of the considered magnitudes in the i-th source, $f_i(m)$ and $g_i(r)$ are the probability density distributions of magnitude and distance between the various locations within source i and the site for which the hazard is being estimated, respectively. In other words, $f_i(m)$ represents the recurrence relation, whereas $g_i(r)$ gives the zonation. $P(Z > z|m, r)$ is the probability that an earthquake of magnitude m and distance r will exceed ground motion level z, which is determined from the ground motion prediction equation. Note that integration is done with respect to distance and magnitude, in order to include all possible locations within source i and all earthquakes of magnitudes within the considered range.

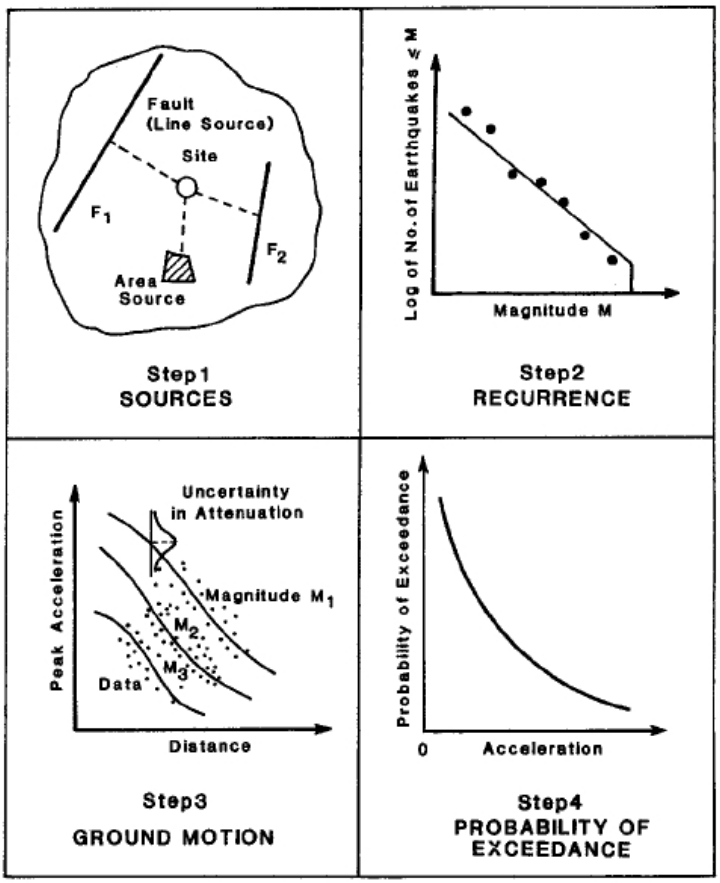

Figure 1.2: Basic steps of probabilistic seismic hazard analysis (after TERA Corporation (1978)).

1.2 Methodologies

Several computer codes are available to perform Probabilistic Seismic Hazard Analysis, some of which are more user-friendly than others. It is important for the analyst

to determine the specific needs in advance, since computer codes exist that are useful for either area or fault source models and some codes are appropriate for creating grids of PSHA values suitable for contouring in ground motion, whereas others can be used to do site-specific analyses (Thenhaus and Campbell, 2003).

1.2.1 Numerical approach of the analytical equations

The aim of this study is to produce seismic hazard maps for the Netherlands, a region that is more suitable for defining area sources instead of fault sources. Commonly used computer codes that are appropriate for this type of analysis are EQRISK (McGuire, 1976) and SEISRISK III (Bender and Perkins, 1987). Less well-known computer programs are FRISK88M (Risk Engineering, 1996) and CRISIS99 (Ordaz, 1999), but the results are similar to those of EQRISK and SEISRISK III (Grünthal, 1999; Atakan et al., 2001). All these programs are numerical approaches to the probabilistic seismic hazard analysis method as presented by Cornell (1968), which is shortly described in the theory section.

For this study, the Cornell-McGuire approach is applied, using the program EQRISK. This is a Fortran 77 program, initially written by McGuire (1976) and modified by Mayer-Rosa and Merz (1976). The program evaluates hazard for each site-source combination and intensity level by numerical integration of equation 1.4. The program needs an input file (seismicity model) containing information about seismic zonation, ground motion prediction equation (and its standard deviation), the magnitude-frequency relation parameters and upper and lower magnitude boundaries. Note that some ground motion prediction equations use a ten-base logarithm and uncertainty values are given as a ten-base logarithm in the literature. Calculations in the program, however, are done in terms of natural logarithm. This is corrected for in the computer code and standard deviation should therefore be converted to natural logarithms as well.

Originally, the program uses a cartesian coordinate system that requires coordinates to be given in kilometers. However, the hazard maps are produced using GMT, which requires conversion to a latitude and longitude coordinate system. In order to avoid unnecessary efforts in later stages of the study, a conversion from cartesian to spherical coordinates is implemented in the program and input coordinates are converted to longitude and latitude values as well.

The advantage of using EQRISK is that it is very easy to include other (relatively simple) ground motion prediction equations in the program. Also, since the program numerically integrates the analytical equations, the result should be very similar to the analytical solution. However, there are some restrictions on the input data; for example, the minimum and maximum magnitudes cannot be chosen independently: at some point in the calculations the probability is being multiplied with a term ($ANEQ$), which is given by

$$ANEQ = \frac{1 - e^{-\beta(M_{max} - M_{min})}}{e^{-\beta M_{min}}\left(1 - e^{-\beta(M_{max} - 2M_{min})}\right)}$$

When $M_{min} = M_{max}/2$ the denominator of this term becomes zero, resulting in infinite hazard values. Taking $M_{min} > M_{max}/2$ results in a negative denominator and the hazard will also be negative, which is not realistic. In order to avoid this problem, it is important to make sure that the lower magnitude bound is smaller than half the maximum magnitude. It is even better to hold on to minimum magnitudes that satisfy $M_{min} = M_{max}/2 - 1$, since values closer to $M_{max}/2$ are already

going to infinity. Since the program is originally developed for active seismic regions where M_{max} is usually much larger than M_{min}, this should not be a problem. However, for low-seismicity areas, such as the Netherlands, magnitude ranges will become very small, due to low maximum magnitude values. Unfortunately, it is not clear why this $ANEQ$ term is implemented in the program and solving this problem is beyond the scope of this thesis. It is strongly recommended to investigate this in further studies.

Another problem that raises in EQRISK is caused by the choice of a strict or loose lower magnitude bound. A strict lower bound means that no events having a magnitude smaller than the minimum magnitude are taken into account, whereas a loose lower bound implies extrapolation to magnitude zero. One would expect that this would make no difference, because small magnitudes are not thought to significantly affect the hazard. However, tests have shown that the hazard increases to unlikely high values when a loose lower bound is used and it is therefore recommended to use a strict lower bound. Although the source code is available, it is very difficult to find out whether numerical problems occur and what causes them. Making the program more suitable for low-seismicity areas would imply that the code should be more or less rewritten. In the next paragraph another program will be discussed, which is particularly developed for low-seismicity regions.

1.2.2 Monte Carlo approach

An alternative method to approach the probabilistic seismic hazard is Monte Carlo simulation. The M3C hazard software, developed by Musson (2009), can be used for both site studies and hazard mapping, particularly in low-seismicity areas. Similar to EQRISK, a seismic source zone model is required as input. Using a Monte Carlo process, the model generates artificial earthquake catalogues, each representing a version consistent with past behaviour on which the model is based. Seismicity parameters such as rate of occurrence and proportion of large to small earthquakes, as well as regional variations in activity are preserved; the actual earthquake locations and time, however, are different. For each site, the ground shaking is estimated, using a ground motion prediction equation.

If a large amount of catalogues is simulated, the probability of occurrence of a given ground motion can be directly estimated from the number of times this ground motion level is exceeded as a proportion of the total number of simulations. The calculations involved in this software are not very complex and it is easy to understand what is going on. Also, more tools (such as the possibility to smoothly taper off the magnitude-frequency relation towards the maximum magnitude) are available in M3C with respect to EQRISK and it offers the possibility to specify uncertainties and limits on these uncertainties. Another advantage of this method is that it is particularly developed for low-seismicity areas and has been tested and debugged before.

On the other hand, the main disadvantage of M3C is that one is always estimating, rather than calculating, the seismic hazard. Although the numerical method is also an approach of the analytical equations, it still actually calculates the hazard for discrete intervals. In the Monte Carlo approach, equation 1.4 is not calculated at all, but the accuracy of the estimation will increase when more simulations are performed. Another disadvantage of using M3C is that the source code is not available. Including ground motion prediction equations, other than those already present in the program, is therefore not possible. Also, when strange features occur in the results, it is very difficult to recover errors.

Chapter 2

Input models

The input model for PSHA requires definition of earthquake sources, seismicity and ground motion prediction equations for the area of interest. The specification of an input model always involves uncertainties and it is very important to bear in mind what these uncertainties are and to analyse the sensitivity of the hazard estimate to different input parameters.

The data, on which the input models are based, come from the earthquake database of the Royal Netherlands Meteorological Institute (KNMI). The dataset contains 261 events, of which the oldest occurred in 1692. All events that occurred since 1906 have been recorded instrumentally (Royal Meteorological Institute of the Netherlands (KNMI), 2010b,a), whereas older events are taken from historical sources. Only earthquakes close enough to the Netherlands to affect the country are taken into account; these events mainly occurred in the Netherlands, Germany and Belgium, and a few in France and the North Sea. In order to make the Poisson assumption valid all known aftershocks are removed from the dataset, using the criterium that an event is an aftershock when

$$\sqrt{r^2 + (ct)^2} < 75 \tag{2.1}$$

where r is the distance from the main shock, t the elapsed time after the main shock and $c = 1\ kms^{-1}$. Events are neither used for which no magnitude or location is available, nor earthquakes that have no natural cause.

2.1 Source zones

Earthquake sources that are activated by tectonic forces are called seismotectonic sources. It is therefore reasonable that this type of sources mainly occurs in regions of high tectonic activity, such as subduction zones or orogens. Earthquake activity concentrates at plate boundaries, as shown in figure 2.1. In those active tectonic regions localization of faults that cause earthquakes is often very accurate, due to the high rate of occurrence of events and the fact that relatively much research is performed. Sources in such regions are therefore primarily defined as line source, which is a map-view representation of three-dimensional fault planes (Thenhaus and Campbell, 2003).

However, natural earthquakes can also occur in stable continental interior regions such as north-western Europe. Such intraplate earthquakes are often caused by small faults, resulting in low magnitude earthquakes. Localization of small individual active faults is not always possible and often zones of faults occur instead of

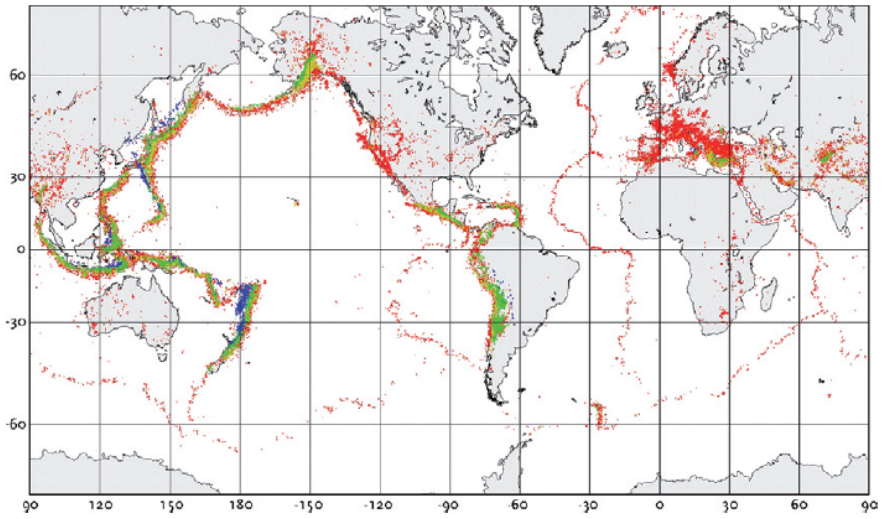

Figure 2.1: Seismicity in the world. Red circles: $0 - 33$ km depth; yellow circles: $30 - 70$ km depth; green circles: $70 - 300$ km depth; blue circles: $300 - 700$ km depth. Source: USGS.

particular large faults. Sources are therefore primarily defined as area sources. Based on different types of geological, geophysical and seismological data, area source zones are described as a region (often a particular geological structure) of uniform seismicity characteristics, which are different from surrounding regions. The earthquake occurrence for a given magnitude is assumed to be uniformly distributed within the source. Usually, earthquake occurrence is only considered between a minimum magnitude of engineering interest (*i.e.* minimum magnitude believed to produce significant ground motion that might cause damage) and a maximum magnitude that is representative for the geological setting. In a region where no large faults are present, it is very unlikely for large earthquakes to occur and taking larger magnitudes into account would give an overestimation of the seismic hazard. The choice on these upper and lower bound magnitudes will be discussed in section 2.5.

It is important to note that the definition of area sources is very subjective. Often, it is difficult to determine whether geological features are active and seismicity cannot always be coupled to faults. It is the task of the analyst to decide which factors are used to determine the boundaries of a source zone. Also, even when fault dimensions would be perfectly known, it is difficult to make an estimation of the seismic movement. Stress along a fault can be released in both seismic and a-seismic movement, which means that not all movement results in an earthquake. The total movement in history can be easily estimated, but it is still very difficult to determine what proportion of that movement was of seismic nature.

After seismic source zones have been defined, the final result is a so-called seismotectonic model. This includes the geographic distribution of seismic sources, rate of occurrence of events and the specification of all source characteristics required for the hazard analysis. Usually, the spatial earthquake occurrence is described up to a maximum distance beyond which the sources have no effect and to a maximum depth earthquakes can occur. This final seismotectonic model is input to the seismic hazard analysis.

As stated earlier, the Netherlands, as well as the surrounding countries, is a low-seismicity area. Although these countries are not situated close to plate boundaries, some small to moderate tectonic earthquakes occur due to the presence of a stress field in this region. The stress field is a consequence of both the spreading at the Mid-Atlantic ridge and the subduction of the African plate beneath the Eurasian plate. Oceanic spreading occurs in south-eastern direction, whereas the northly directed subduction causes forces that are mainly absorbed by the Alps, but some reach further north. This results in a stress field with compressional forces trending in a southeast-northwest direction. As a consequence, extension occurs in the perpendicular (SW-NE) direction. Intra-plate faults are most likely to develop at places where the crust is relatively weak.

This extensional stress regime is reflected in the Rhine Graben Rift System as shown in figure 2.2. Perpendicular to the direction of tensional forces normal faults are present, along which subsidence of the graben occurs. Also, strike-slip faults are present, which are caused by shear stresses with an orientation between that of the extensional and compressional stresses. The Rhine Graben System can be classified in several branches: the Upper Rhine Graben, the Lower Rhine Graben, the Hessian Graben – although displaying little neotectonic activity – , and the Belgian Brabant Massif region. The northern part of the Rhine Graben System mainly consists of normal (antithetic and synthetic) faults, whereas in the Upper Rhine Graben and the Belgian (Brabant) Zone strike-slip faults are dominant (Ahorner, 1983b). The dominant strike-slip fault in Belgium is the Bordière fault (see figure 2.2). More or less parallel to this fault, slightly more to the southeast, the Midi-Eifel-Aachen thrust complex is located. South of the western part of the Bordière fault is a shear zone, which is called the North Artois Shear Zone (Leynaud et al., 2000).

The northwestern branch of the Rhine Graben System, the Lower Rhine Graben (LRG), is formed by the Roer Valley Graben (figure 2.3), which is the most prominent tectonic feature in the Netherlands. This graben consists of several normal faults. The dominant faults of the Roer Valley Graben are the Peel boundary fault and the Feldbiss fault, respectively. These faults are surrounded by smaller normal faults, such as the Rauw fault. During the late Oligocene, differential subsidence of the Roer Valley Graben along these faults started (Geluk et al., 1994) and it still continues.

The zonation used to represent the seismicity in the area of interest is based on the source zone models described by Leynaud et al. (2000) and Hinzen (personal communication), which partly overlap. The zonation models are shown in figure 2.4 and 2.5, respectively. The zones defined by Leynaud et al. (2000) mainly consider seismicity in Belgium and only small parts of Germany, whereas the model of Hinzen extends more to the south-east of Germany. Since the aim of this research is to investigate the seismic hazard for the Netherlands, events in both Belgium and Germany should be considered and therefore a combination of both zonation models is used. However, source zones that are located too far south or east from the Netherlands are not taken into account; only earthquakes of magnitudes that are unlikely to occur in this part of Europe would be large enough to affect the Netherlands.

The final result of the zonation used for this study is shown in figure 2.6. For the Belgian part of the area the zonation defined by Leynaud et al. (2000) seems to make more sense than that of Hinzen. For example, the southern boundary of the Belgium Shear Zone is defined by the large strike-slip Bordière fault shown in figure 2.2. The Hainaut Zone is characterized by a relatively high and shallow

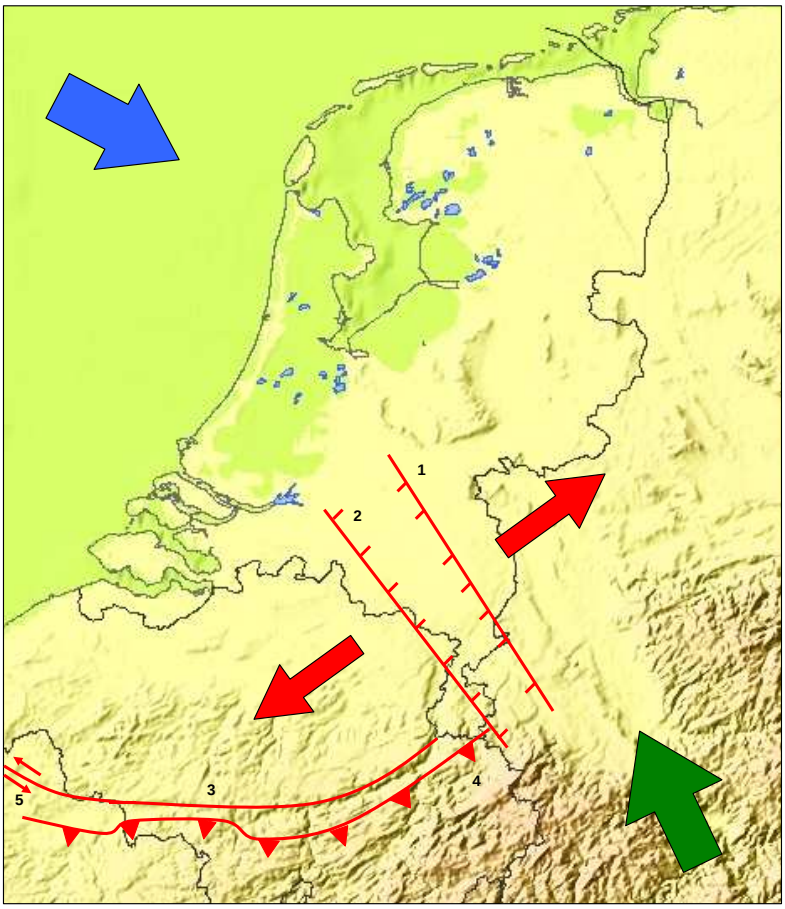

Figure 2.2: Schematic representation of the Rhine Graben System. 1: Peel Boundary Fault, 2: Feldbiss Fault, 3: Bordière Fault, 4: Midi-Eifel-Aachen Fault, 5: North Artois Shear Zone.

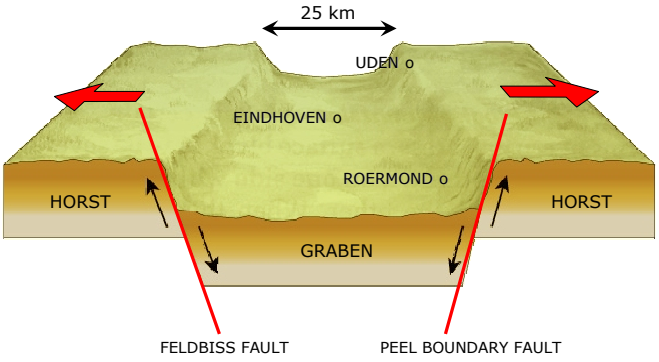

Figure 2.3: Section through Roer Valley Graben.

seismic activity. Hinzen has combined these clearly different zones into one zone. Also the Liège zone, which is characterized by shallow events cannot be clearly distinguished in the model of Hinzen. The Roer Valley Graben (RVGC), however, is similarly defined by both authors; the zone is delineated in the northeast by the Peel Boundary Fault, whereas the southwestern boundary is the Feldbiss Fault. The smaller normal faults surrounding the graben are characterized by relatively small magnitudes. Therefore two distinct source zones are added northeast and southwest to the Roer Valley Graben. Note that the zone northeast of the Roer Valley Graben was not included by Leynaud et al. (2000). However, since in this area events occurred that affected the Netherlands, the zone is considered in this study.

A description and motivation for the choice of each zone is given below.

1. Neuwied Basin zone (NEUB): This area is clearly distinguishable from the surrounding areas, since the stress field and focal depths of events are clearly different (Hinzen, 2003; Ahorner, 1983a). Stress drops have been shown to be unusually low in the Neuwied Basin (Ahorner, 1983a) and focal depths are smaller than in the surrounding zone (*i.e.* 10 km).
2. Germany zone (GERM): This zone partly covers the Rhenish Massif. Mainly normal faults occur, at focal depths that are predominantly larger than those of events in the Neuwied Basin (15 km).
3. Central Roer Valley Graben zone (RVGC): As stated earlier, the western and eastern boundaries of this source zone are defined by the Feldbiss fault and the Peel Boundary fault, respectively. Since these are normal faults, dipping towards each other, events caused by any of these faults always occur in between. This zone is characterised by relatively high seismic activity, with large events and large focal depth. The northern boundary is defined by

the limit of the graben structure, which is found from a gravimetry map (Camelbeeck, 1994). The southern boundary is fixed where no seismicity has been measured.

4. Western Roer Valley Graben zone (RVGW): The Central Roer Valley Graben zone is surrounded by several small normal faults, which cause events that occur at similar focal depths, but are significantly smaller than those in the Central Roer Valley Graben zone. It is therefore not realistic to combine the faults into one zone and it was decided to define a distinct zone to the southwest of the Feldbiss fault. The northern part of this zone is again defined by the limit of the graben structure (Camelbeeck, 1994), whereas the Rauw fault defines the western boundary. Both seismicity and geology validate the same choice in this area.
5. Liège zone (LUIK): This zone is delineated to the east by the Central Roer Valley Graben zone. It is included as a separate zone, because it has a high seismic activity and faults dominantly have strike-slip or thrust instead of normal components. The northern boundary of the zone is defined by the Bordière fault, whereas the Midi-Eifel-Aachen thrust complex is the southern boundary. Because two different kinds of fault mechanisms are present in the zone, events occur both at a shallow depth (at Voerendaal and Liège), due to the strike-slip fault, as well as at large depth, caused by the thrust complex. One could subdivide this zone into two zones, each having a different focal depth, but the amount of data is insufficient in order to do an appropriate analysis. Since the events that occur at large depth have small effect, relative to the shallow events, the depth is taken to be 5 km.
6. Hautes Fagnes zone (HOVE): Similar to the Liège zone, the Hautes Fagnes zone is characterized by a high seismic activity. However, besides strike-slip faults, also normal faults occur in this region. Furthermore, the estimated focal depths are, respectively, larger and smaller than those in the Liège zone and the Roer Valley Graben.
7. Belgian Brabant Massif zone (BBMZ): This part of the Brabant Massif contains several Paleozoic faults that have caused (relatively small) earthquakes in the past. The southern boundary of the zone is defined by the Bordière fault, which extends from the west of Belgium to the Roer Valley Graben. This fault dips to the north, so no earthquakes will occur to the south of the fault. Furthermore, northwest-southeast trending geophysical anomalies have been measured in this area (Leynaud et al., 2000). Based on these anomalies and seismicity, the northern boundary of the zone is defined as shown in figure 2.6.
8. Hainaut zone (HAIN): This zone is specifically based on seismicity data. Although no clear faults are present (except for a small part of the Bordière fault), it seems to be clear from the seismicity data that this is a distinct zone. Significantly more and shallower earthquakes have occurred in this region than in surrounding areas. Ahorner (1983a) suggests that the shallow seismicity is caused by collapsing cavities in evaporites and accompanying shear dislocations in the overlying material.
9. North Sea zone (NSEA): During the Middle Ages three large and deep shocks occurred in this zone, which were felt in the Netherlands. Since no significant seismicity has been measured ever since, the zone is included with a very low seismicity rate. Little is known about the geology of this area; the events could correspond to a graben structure, but the dimensions are unknown.

10. Eastern Roer Valley Graben Zone (RVGE): For the same reason the Western Roer Valley Graben zone was defined, also a source zone is added to the east of the Central Roer Valley Graben zone. The rate and magnitudes of events in this area are significantly lower than in between the Feldbiss fault and the Peel Boundary fault. Since this study only considers tectonic earthquakes, the zone is defined in such a way that the induced events, which are caused by mining in Germany, are not included.

Note that this seismotectonic zone model is very subjective. The best example to illustrate this is the Belgian Brabant Massif Zone. From seismicity and geophysical data one would conclude that this zone should be defined as shown in figure 2.6. However, there is no geological indication for the northern boundary to be like this. The Brabant Massif, which is the main geological feature in this region, extends much further north and no faults are known to be present at the location of the northern boundary in figure 2.6.

The Roer Valley Graben is delineated by the two major faults in this area and surrounding faults are part of other source zones, east and west from the Roer Valley Graben. There is still discussion going on about whether this is a right choice. It might be better to include all faults into one single zone, but, on the other hand, the maximum magnitude is clearly lower for the surrounding regions. At some point one has to choose one of the alternatives and bear in mind how this affects the hazard estimate. Section 2.5 discusses the sensitivity of the hazard estimate to different zonation models in further detail.

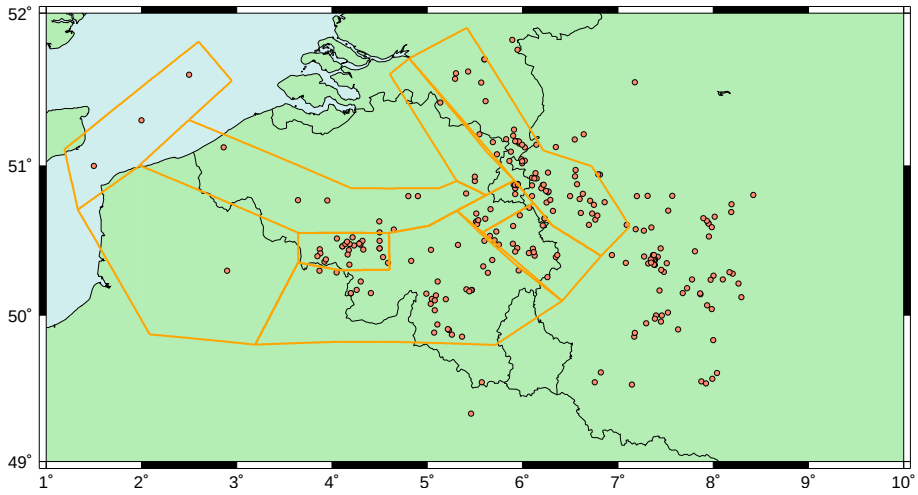

Figure 2.4: Source zones after Leynaud et al. (2000); orange circles represent the location of earthquakes.

2.2 Seismicity characterization

As stated earlier, the seismicity can be characterized with the Gutenberg-Richter relation (recurrence relation):

$$Log\ N = A - BM$$

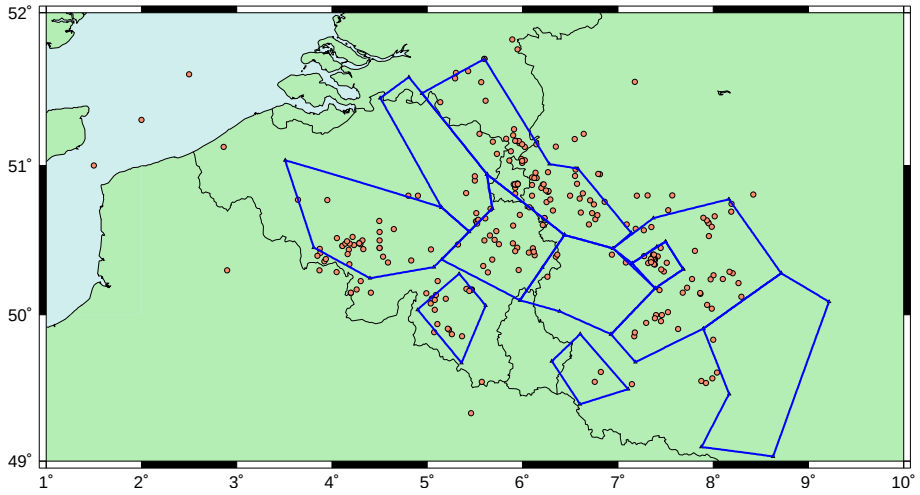

Figure 2.5: Source zones (only the zones that would affect the Netherlands) after Hinzen (personal communication); orange circles represent the location of earthquakes.

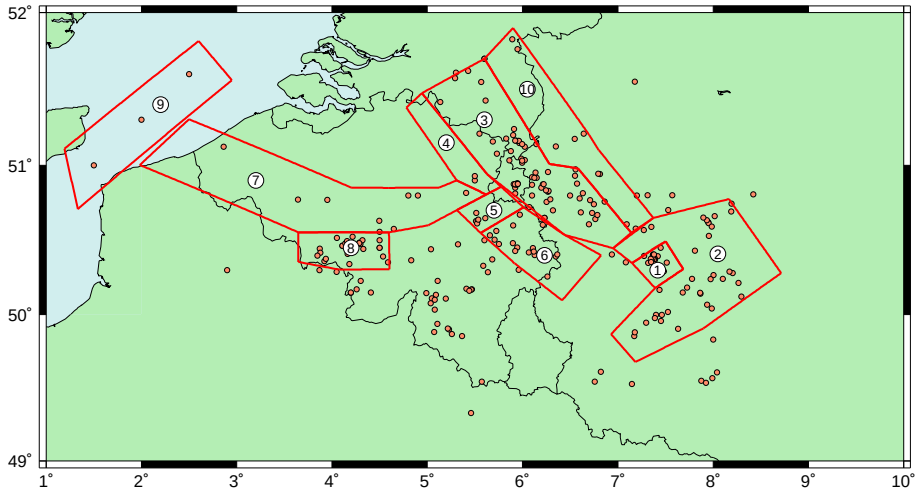

Figure 2.6: Final zonation model used for seismic hazard analysis, which is a combination of the models of Leynaud et al. (2000) and Hinzen; orange circles represent the location of earthquakes. 1: Eifel zone (NEUB), 2: Germany zone (GERM), 3: Central Roer Valley Graben zone (RVGC), 4: Western Roer Valley Graben zone (RVGW), 5: Liège zone (LUIK), 6: Hautes Fagnes zone (HOVE), 7: Belgian Brabant Massif zone (BBMZ), 8: Hainaut zone (HAIN), 9: North Sea zone (NSEA), 10: Eastern Roer Valley Graben zone (RVGE).

For this study, the constants A and B in this relation are determined from the earthquake catalogue of the Netherlands and surrounding countries. Both a maximum likelyhood regression technique and a Monte Carlo approach were applied, which resulted in similar values for the parameters. Only data of events with a magnitude larger than 2.5 are used for the regression, in order to make sure the dataset is complete. Smaller magnitudes are not always recorded and taking those into account would give unreliable results. For further modelling the results of the Monte Carlo simulation are used.

A gives the rate of occurrence of events larger than a certain magnitude (intercept of the curve of the sum of all zones) and B gives the relative distribution of small and large events, or the slope of the line. Due to the small dataset available, determination of B for each zone separately would result in a very high uncertainty of the fitted line. Therefore, a constant B is determined from the whole dataset, which will be applied to each zone. A is determined for each zone separately in such a way that the sum of all individual rates equals the total amount of events from the entire area. For moment magnitude the values for A and B are found to be 2.87 ± 0.22 and 0.90 ± 0.04, respectively. When calculations are performed in terms of local magnitude, the values are respectively 2.66 ± 0.14 and 0.77 ± 0.03. Since most ground motion prediction equations are based on moment or surface wave magnitudes ($M_S \simeq M_W$ for the magnitude range of the earthquake catalogue), the values that were determined for moment magnitude will be primarily used. Only when a ground motion prediction equation using M_L is used, the other values are input.

The maximum magnitude for each zone is also determined by means of the earthquake catalogue. In each zone a maximum magnitude that has ever been recorded can be found. Because it is not inconceivable that an earthquake larger than this magnitude could occur, the maximum magnitude ever recorded is thought to be the 'minimum maximum magnitude'. For the Netherlands, the ultimate maximum magnitude for the whole area is determined by using a Monte Carlo method, resulting in a value of $M_W = 6.2 \pm 0.2$, or $M_L = 6.3 \pm 0.2$. Taking larger events into account would be unrealistic. Unfortunately, not enough data are available to estimate the maximum magnitude for each zone separately by using this method. For zones that clearly contain smaller magnitudes than $M_W = 6.2$, the upper magnitude bound is chosen to be half a unit of magnitude larger than the largest event that has ever been recorded in the zone. Obviously, due to errors in the determination of magnitudes and because it is a rough estimation, there is an uncertainty on this maximum magnitude. For the choice of minimum magnitude, one would expect that it does not strongly influence the hazard estimate, because small magnitudes do not cause damage. As tests have shown, however, this is not always the case. Furthermore, the EQRISK program puts a constraint on the minimum magnitude. The sensitivity of the hazard estimate to the magnitude bounds will be discussed in section 2.5.

2.3 Ground Motion Prediction Equations

Many empirical ground motion prediction (attenuation) equations have been developed over the years. Since attenuation depends on local characteristics of an area (*i.e.* tectonic setting and geological parameters) the empirically determined relations are only valid for similar tectonic environments. For the same reason, data on

which the equations are based usually come from one region where the characteristics are considered to be approximately homogeneous. For low-seismicity areas, however, the available database of strong ground motion measurements is limited and determination of an appropriate ground motion prediction equation is a rather difficult task.

Ground motion prediction equations are determined from a certain data set and for given definitions of source-to-site distance, magnitude scale and local site conditions. Some ground motion estimation relations take fault mechanism and focal depth into account. In the Netherlands dominantly normal fault mechanisms and firm soil or alluvium sites are present, so it is not necessary to use terms considering other soil types in the relationship. Ground motion is usually estimated in terms of Peak Ground Acceleration (PGA), Peak Ground Velocity (PGV) or as a response spectrum. In a response spectrum the apparent ground acceleration or velocity is plotted against frequency; attenuation depends on frequency, so one can read the maximum ground motion caused by a single frequency. Also, the response of an engineering structure is included as harmonic oscillator. For this study, only PGA is considered.

Several recently developed ground motion prediction equations, which could be useful for seismic hazard analysis in the Netherlands, are selected. Selection criteria are data origin, magnitude domain and distance interval. Several studies (Dost et al., 2004; Bommer et al., 2006) show that under-/or overpredictions appear when a relation, based on data with magnitudes within a certain range, is used for events with magnitudes outside that range.

A short summary of the relations that might be interesting for the Netherlands is given in the appendix. Due to the small data sets for northwestern Europe, most of the equations are based on data from a limited amount of countries. In section 2.5 the advantages and disadvantages will be considered, as well as the sensitivity of the hazard estimations to the choice of different relationships. Unfortunately, the M3C program uses other relations than EQRISK (except for those of Berge-Thierry et al. (2003) and Ambraseys et al. (1996)). Most of the relations used by M3C are too complex to insert into EQRISK, whereas it is impossible to include the simpler ones used by EQRISK into M3C as well.

A short summary of the selected ground motion prediction equations is given below, explaining on what criteria they were chosen.

Ambraseys (1995), Ambraseys et al. (1996) and Ambraseys et al. (2005) give a series of empirically determined ground motion prediction equations. All equations are based on data from Europe and the Middle East. Using data from the Middle East is admissable, in contrast to for example Californian data, since there does not seem to be a significant difference in ground motions between the Middle East and Europe, whereas ground motions in California are slightly higher than in Europe for the same magnitude and distance (Douglas, 2004). Although more ground motion data were available, the Ambraseys et al. (2005) study mainly uses data from seismically active regions, resulting in a higher magnitude range. Ambraseys (1995) presents both depth dependent relations and relations considering a constant focal depth. This constant focal depth term (h_0) accounts for the fact that the closest point on the surface projection of the fault, or from the epicentre, is not necessarily the source of the peak motion and it does not represent explicitly the effect of the depth on the acceleration. However, as will be shown in section 2.5, results are comparable to those of a depth-dependent equation using h_0 as focal depth. Therefore, h_0 can be interpreted as a mean focal depth for the entire region

of interest. In the other two studies the source-to-site distance is defined as the closest distance to the surface projection of the fault rupture (Joyner and Boore, 1981). Again, a constant term h_0 is present in the distance dependent term of the equations. Horizontal distances used are in the order of a few hundred kilometers, which is appropriate for this study. The depth dependent relation presented by Ambraseys (1995) was also used for a seismic hazard study in Belgium (Leynaud et al., 2000). The results will be compared to those of this study later.

Another series of ground motion estimation equations has been developed by Campbell (1997), Campbell and Bozorgnia (2003) and Campbell and Bozorgnia (2008). Although the relations are based on data from all over the world and developed for shallow seismically active regions in North America (data from stable continental regions are exluded in Campbell and Bozorgnia (2008)), the magnitude-/and distance ranges are appropriate for the Netherlands. Source-to-site distance is defined as the shortest distance between the recording site and the zone of the seismogenic energy release on the causative fault, which is depth dependent. Note that the relation presented in Campbell and Bozorgnia (2008) is from the Next Generation Attenuation (NGA) project, which is much more complex than the older equations.

Another more complex relation was designed for intraplate earthquakes in Eastern North America by Atkinson and Boore (2006). The magnitude and depth range are appropriate for the Netherlands, but distances of significance for seismic hazard assessment in northwestern Europe are much smaller than distances used in this study. In contrast to the other studies, this ground motion prediction equation is not empirically determined, but it is a theoretical model.

Berge-Thierry et al. (2003) presented a ground motion relation, applicible for shallow earthquakes in France, which is particularly based on records selected from the European Strong Motion (ESM) database; only a few American records are added to the dataset in order to get an appropriate magnitude distance distribution applicible over a large magnitude range. The relation takes focal depth into account and magnitude and distance ranges are appropriate for the Netherlands. Coefficients for the attenuation relation are given for a range of frequencies (response spectrum). Since the ground motion relation won't change significantly for a frequency of 33 Hz when another damping factor is chosen, the coefficients corresponding to this frequency are used for this study.

Based on European and Southwest Asian data, a ground motion prediction equation was developed by Bommer et al. (2006). The interesting thing about this model is that it includes input data from events as small as 3.5 M_W and distance range is up to 100 km. Similar to the relations presented by Ambraseys et al. (1996) and Ambraseys et al. (2005), the equation of Bommer et al. (2006) does not take focal depth into account.

The only ground motion prediction equation particularly developed for the Netherlands is presented in Dost et al. (2004). Considered data are measured by accelerometers, situated in different parts (mainly the northern and south-eastern part) of the Netherlands. The study concentrates on very low magnitudes and therefore small source-to-site distances. Both recordings from tectonic and induced events are used to estimate the ground motion relation. Due to the small amount of data used, the uncertainty on this relation is relatively large. Also, the depth and magnitude of the events used are very small; the depth range is up to 5 km, and magnitudes range from 2.3 up to 3.9. Although such events do occur in the Netherlands, they are not representative for the Roer Valley Graben. When applied to

larger magnitudes, the relation gives an overestimation of the PGA (Dost et al., 2004). Although the other ground motion prediction equations are not based on representative data as well, it is usually better to use a regional relation, which has a small uncertainty due to the large amount of data, than to use a local relation with a large uncertainty.

2.4 Local site effects

As stated earlier, the material through which seismic waves propagate can strongly influence ground motion attenuation, especially at local scale, close to the receiver (*i.e.* the upper $30 - 100$ m). It is therefore important to include knowledge of soil properties of the site in the hazard analysis.

Due to the higher resistance of particle motion, wave amplitudes are decreased when the impedance is increased. Impedance can be defined as the product of density and shear wave velocity (Reiter, 1990), so ground motion produced by events of equal source and distance will be larger at sites of low velocity and density (*e.g.* soft soil or alluvium) sites than at sites consisting of hard rock (high velocity and density). On the contrary, absorption, which reduces the seismic wave amplitude, tends to be greater on soft soil than on hard rock sites. The balance between the impact of impedance and absorption depends on the frequencies of the wave.

The wave amplitude is also affected when crossing an interface; large impedance contrasts usually increase the amplitude of upcoming waves. Again this increase in ground motion can be counteracted by the fact that part of the wave energy is converted to other wave types when tranmitting an interface. Also, reverberation can occur in the upper layer, which may (depending on frequency and phase) result in resonance.

Site conditions are implemented into seismic hazard analysis through the $f_4(P_i)$ term in ground motion prediction equation 1.2. Site conditions are usually defined as broad categories, such as soft and stiff soil, alluvium, or rock. Sometimes the classes are determined by means of shear wave velocity, which is higher than approximately 2000 m/s for hard rock sites. In the Netherlands and surrounding countries, no hard rock is present, but mainly stiff soil. The options for site conditions that can be chosen are different for various ground motion prediction equations; in this study ground motion prediction equations are chosen that are suitable for firm/stiff soil, or alluvium. For this moment, there is insufficient knowledge and no possibility in the computer codes to include this parameter in a more detailed way. Soil conditions are therefore taken to be similar through the entire region.

2.5 Uncertainties

Seismic hazard analysis admits to a wide range of interpretations and uncertainties (Thenhaus and Campbell, 2003); there are two types of uncertainty. Since predictive models are usually subjective for a certain extent, due to lack of knowledge, there is always some uncertainty, which is called epistemic uncertainty. When a model would be perfectly correct, the variation in the predicted parameter is a consequence of uncertainty in the data, resulting in aleatory variability. So, improving the model would reduce epistemic uncertainty, whereas aleatory variability can be reduced by using more data, but will always be present.

Several tests are performed, in order to do a preliminary analysis of the sensitivities of the hazard estimate to different parameters. In both programs it is impossible to specify uncertainties for each single parameter. In EQRISK only aleatory variability on the ground motion prediction equation can be given and in the M3C program uncertainties can be specified for the A and B values of the recurrence relationship, maximum magnitude and epicentral scatter. The aleatory variabilities of the ground motion prediction equations are built in the program.

In order to reduce calculation time, many tests were performed on a small domain, covering part of the Roer Valley Graben. For these tests only one zone (RVGC) has been considered. For varying parameters and uncertainties sections are made through the area, at a latitude coordinate of 51.1°. When possible, the tests are performed in both EQRISK and M3C. It is therefore useful to first compare both programs, using the same input as far as possible. Figure 2.7 shows the results for the same ground motion prediction equation (*i.e.* Berge-Thierry et al. (2003)) and equal minimum and maximum magnitude, depth and seismicity parameters in both programs. The results from M3C are slightly higher (less than 10%) than those of EQRISK. For this reason, and also because most ground motion prediction equations are available in only one of the codes and there are constraints on the input for EQRISK, it is difficult to compare both programs. When necessary, sensitivity will therefore be tested for each program separately.

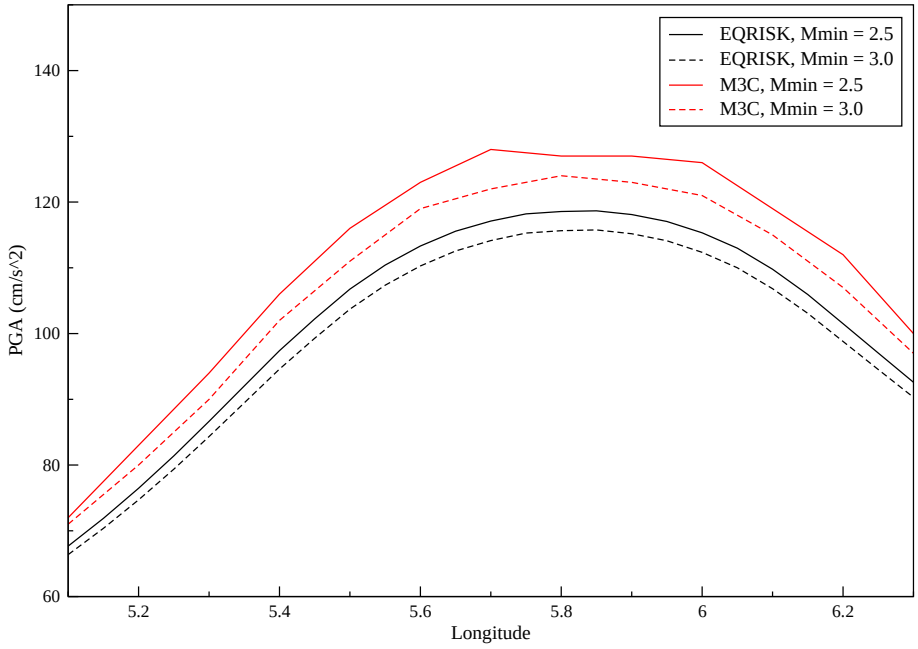

Figure 2.7: Results of two runs, using equal parameters, in both EQRISK and M3C.

2.5.1 Ground motion prediction equation

For ground motion prediction equations, uncertainty can clearly be subdivided into aleatory and epistemic uncertainties. The first is the uncertainty in the data used in the analysis to derive the equation; aleatory uncertainty is usually specified as

the standard deviation of the ground motion relation. Epistemic (modelling) uncertainty, on the other hand, can be modeled by comparing results of different ground motion prediction equations.

In section 2.3 several ground motion prediction equations that might be suitable for the area of interest have been discussed. Many factors, such as magnitude and distance range (epicentral or hypocentral distance), as well as the source area of the data, determine how well a relation suits the Netherlands. It is very difficult to determine which relation would be the best choice to use for the Netherlands at once, so each parameter of influence will be discussed separately.

When plotting the relations, it turned out that the ground motion prediction equation proposed by Atkinson and Boore (2006) gave results that are very different from the other relations (see figure 2.8). According to Atkinson and Boore (2006) a new analysis of eastern North-American data has revealed that geometric spreading is significantly faster at near-source distances ($< 70\ km$) than was determined in previous studies. At distances between 70 km and 140 km the amplitude is supposed to increase, due to Moho bounce effects. At even larger distances the amplitude decreases again, but not as fast as at near-source distances. This results in the irregular shape of the curve shown in figure 2.8, which is only the case for the relation presented by Atkinson and Boore (2006); all other relations have a curve similar to that of Dost et al. (2004). For this reason, and because there is no consensus yet whether this is also a good theory for the Netherlands, this ground motion prediction equation is not used in this study.

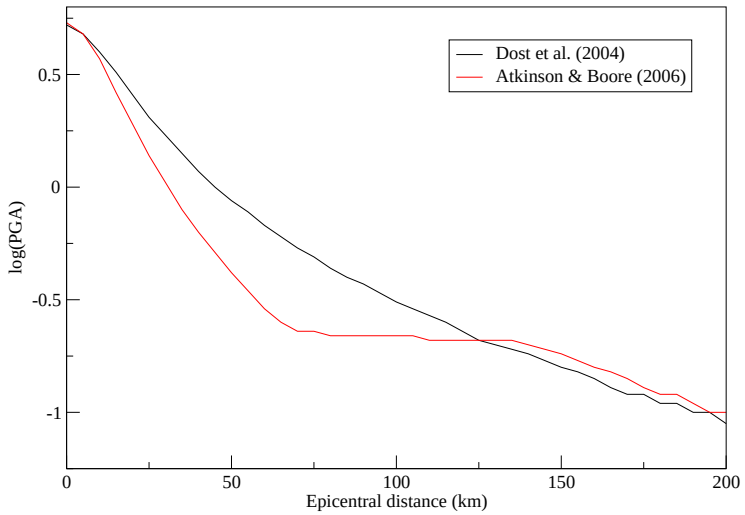

Figure 2.8: Peak Ground Acceleration given by ground motion prediction equations of Dost et al. (2004) and Atkinson and Boore (2006). A fixed magnitude ($M = 3$) and depth ($h = 15\ km$) are used.

Tests have shown that the main differences between ground motion prediction equations are caused by the way the relations treat focal depth and minimum magnitude. Therefore, the sensitivity of the hazard estimate to these two param-

eters will be discussed in the next paragraphs, which forms the foundation of the choice on ground motion prediction equation.

2.5.2 Focal depth

After some runs were performed, by each time varying one single parameter, it turned out that the hazard estimate is strongly sensitive to focal depth (at least when a depth-dependent ground motion prediction equation is used). The results for both EQRISK and M3C are shown in figure 2.9. Note that the results of M3C have lower acceleration values than those of EQRISK. This is in contrast with the comparison done earlier (see figure 2.7), but will be explained later.

From figure 2.9 it can be concluded that for larger focal depths, the hazard estimate decreases, and vice versa. In fact, this result is not very surprising; one would expect that seismic waves, which are generated by deeper sources and thus have travelled a larger distance, cause smaller accelerations. The complication is that some ground motion prediction equations consider hypocentral distance and take focal depth into account, whereas others do not. In figure 2.10 the ground motion prediction equations presented by Bommer et al. (2006) and Campbell and Bozorgnia (2008) are used to plot a section of PGA for different focal depths. The first equation only considers epicentral distance, using a constant term of $h_0 = 8.0282\ km$, whereas the latter takes focal depth into account. It is clear that the depth dependent relation is most similar to that of Bommer et al. (2006), when the focal depth is equal to the constant term h_0. In other words, h_0 actually functions as a mean focal depth for the entire area of interest. For actual focal depths larger than h_0 the depth-independent relation gives an overestimation relative to Campbell and Bozorgnia (2008) and vice versa. Now the question is which one is more reliable; should focal depth be taken into account, or not?

According to McGarr (1984) focal depth clearly is an important factor to be taken into account in the prediction of seismic ground motion. On the other hand, focal depth is often one of the least well-determined parameters in earthquake localization (Ambraseys, 1995). Also, due to the small amount of data, there is a large variation in focal depth estimates of events within one zone. Subdivision of the zones into more zones with less variation in focal depth is not an option, because zones would contain insufficient data in order to do an appropriate hazard analysis. For this reason, together with the fact that uncertainties on depth estimation are large, one could argue that it would be better not to take focal depth into account. However, it is possible to distinguish zones that contain relatively deep events with respect to other zones. For example, the Hainaut zone is characterised with shallow earthquakes, compared to the surrounding areas. Another example is the Roer Valley Graben: in the central region the major part of the events occurred at a depth larger than 10 km, whereas in the areas situated northeast and southwest of the central part the focal depth estimates tend to be much smaller. Therefore, the decision was made to subdivide the zones into 'deep', 'moderately deep' and 'shallow' zones, for which focal depth is estimated to be 15, 10 and 5 km, respectively. Although this is a fairly rough estimation, it seems to be more reliable than assuming that all events occur at the same constant focal depth. A consequence of this decision is that only ground motion prediction equations are left to use that take focal depth into account. This decision is confirmed by the fact that if a relation that contains a constant h_0 term would be used, this term should be similar to the mean focal depth throughout the entire area. This is not the case for any of the selected depth-independent relations, so they are considered to be not suitable for

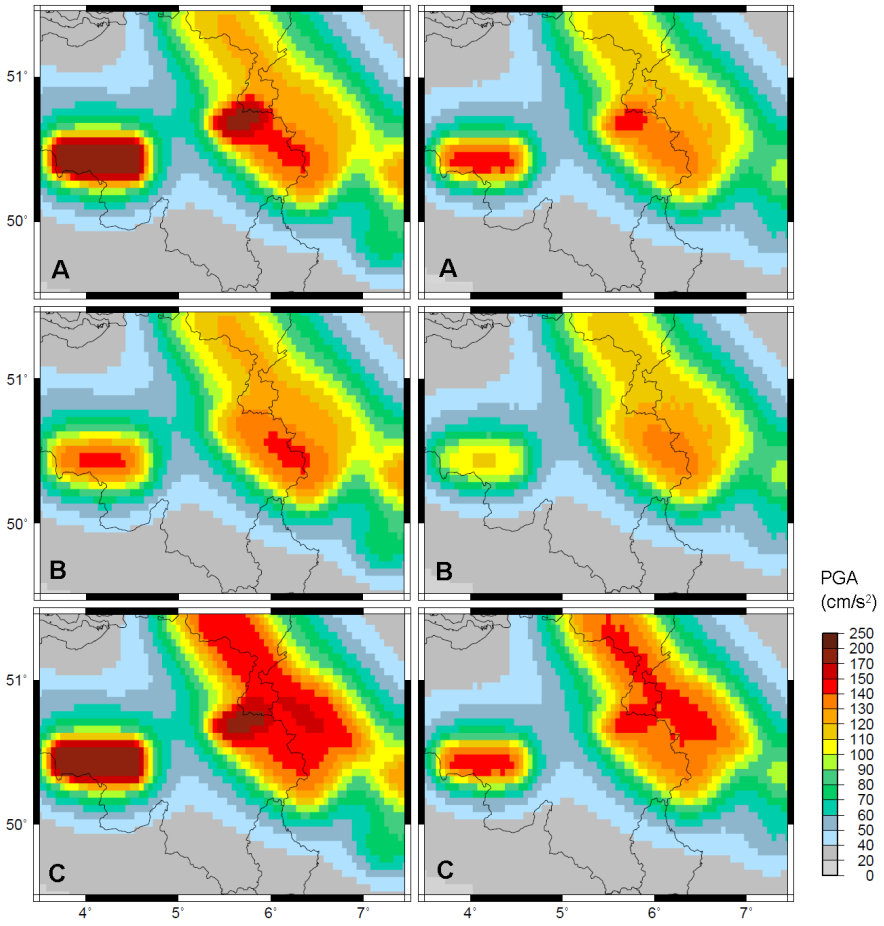

Figure 2.9: Hazard estimates using EQRISK (left) and M3C (right) for various depths. A: Reference map with focal depths as given in table 3.1. B: focal depth of 10 km (instead of 5 km) for Liège and Hainaut zone. C: focal depth of 10 km (instead of 15 km) for Central Roer Valley Graben zone.

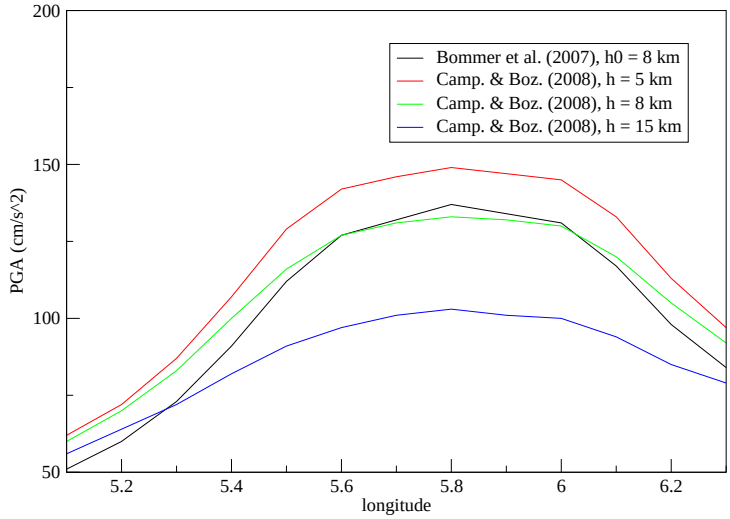

Figure 2.10: PGA values through the test section predicted by a depth-dependent (Campbell and Bozorgnia, 2008) and a depth-independent (Bommer et al., 2006) ground motion prediction equation, for different focal depths.

the Netherlands.

It turned out that focal depth only influences the ground motion prediction for near-source distances. From a certain distance on, the curves of the ground motion prediction equations overlap. For a magnitude of $M = 5$ this distance is approximately 50 km, whereas for smaller magnitudes the curves overlap for even smaller distances. This was found to be the case for each of the selected ground motion prediction equations.

Now all remaining relations are plotted for different focal depths and magnitudes in figure 2.11. It can be concluded that, besides focal depth, the hazard estimate is also very sensitive for the choice on ground motion prediction equation. On top of that, the differences between the ground motion prediction equations depend on the magnitude.

2.5.3 Minimum magnitude

The choice on minimum magnitude is often thought to be of small importance, because it deals with events that are not expected to produce significant ground motions. However, due to their high annual rates, small magnitude events might actually contribute to the hazard estimate.

According to Beauval (2003), the impact of the choice on minimum magnitude mainly depends on seismicity parameters (A and B): the impact decreases with increasing seismic rate (A) and therefore the sensitivity of the hazard estimate is especially high for moderate seismic regions. Increasing the slope of the Gutenberg-Richter relation (B) implies more small earthquakes to occur, which results in a higher sensitivity to minimum magnitude. On the other hand, seismicity parame-

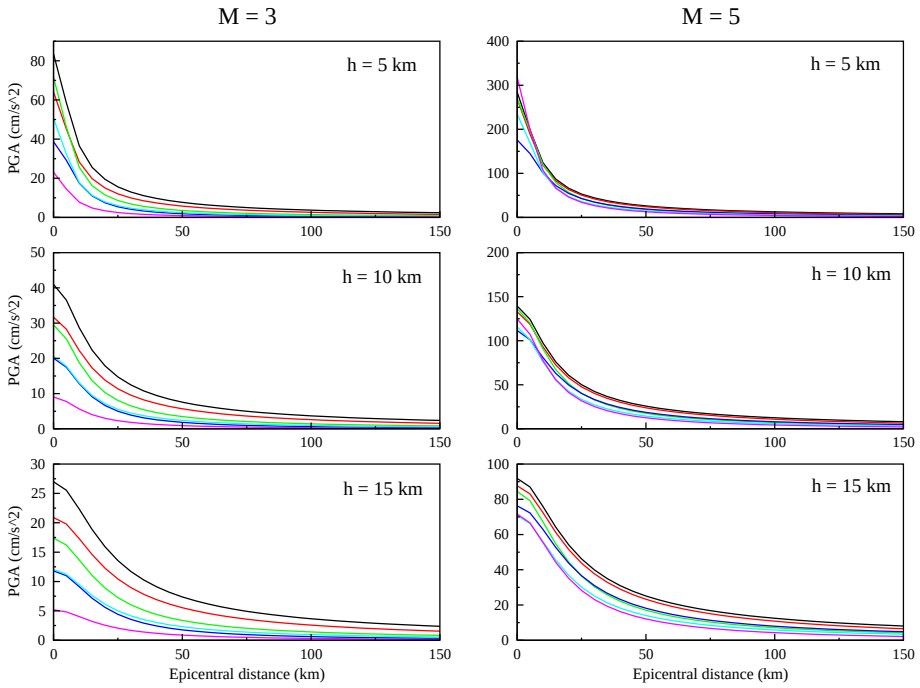

Figure 2.11: Selected ground motion prediction equations for different magnitudes and focal depths. All depth-independent relations, as well as the relation proposed by Atkinson and Boore (2006) are omitted. Black line: Ambraseys (1995); red line: Berge-Thierry et al. (2003); green line: Campbell and Bozorgnia (2003); light blue line: Campbell (1997); dark blue line: Campbell and Bozorgnia (2008); pink line: Dost et al. (2004).

ters also depend on the choice of minimum magnitude. In the determination of A and B, a minimum magnitude (different from that used in the actual calculations) is chosen in order to make sure that the dataset is complete. Chosing this minimum magnitude differently, results in different seismicity parameters.

Several runs are performed, varying the minimum magnitude and the attenuation law. It was found that the impact of minimum magnitude strongly depends on the choice of ground motion prediction equation. The problem in deciding which attenuation relation predicts the PGA in the most reliable way is that actually none of the relations was developed for the entire magnitude range considered in this study. Most of the equations are based on data with magnitudes larger than 4. Bommer et al. (2006) and Dost et al. (2004) state that it is very important to apply ground motion prediction equations at magnitude ranges similar to that of the data on which the relation is based.

The results of tests, using different ground motion prediction equations in EQRISK are shown in figure 2.12. The curves obtained using the relations of Ambraseys (1995) and Berge-Thierry et al. (2003) are not surprising: one would expect that when a larger minimum magnitude is chosen, the hazard estimate slightly decreases, but for minimum magnitudes smaller than 4, this effect should be relatively small (Beauval, 2003). However, the behavior of the other relations (Campbell, 1997; Campbell and Bozorgnia, 2003; Dost et al., 2004), which are all based on the same form (Campbell, 1997), is very unexpected and unrealistic. Whereas most curves are exactly equal for different minimum magnitudes, the curves for $M_{min} = 2.5$ (and that for $M_{min} = 2.0$ of Campbell and Bozorgnia (2003)) are very deviant. Also, the shapes of each curve do not correspond to those of Ambraseys (1995) and Berge-Thierry et al. (2003). For a minimum magnitude of 3.5 or 4.0, however, these artifacts seem to disappear. Unfortunately, it is not possible to do the entire hazard analysis using such high values for minimum magnitude, since the program will give erroneous results at some sites, due to the constraint described in section 1.2.1 ($M_{min} \leq M_{max}/2$).

Performing the same test in M3C results in the curves shown in figure 2.13. A striking phenomenon is that, when using the ground motion prediction equation of Campbell and Bozorgnia (2008), the M3C program crashes for a minimum magnitude smaller than 3.2. Together with the fact that abnormal behavior for small magnitudes was seen in EQRISK for similar relations (the relation presented by Campbell and Bozorgnia (2008) is based on the same form as Campbell (1997), Campbell and Bozorgnia (2003) and Dost et al. (2004)), this suggests that these problems are caused by numerical problems, rather than by the program. Research on this phenomenon is beyond the scope of this study. For now, it is decided not to use any of these ground motion prediction equations in EQRISK, since in that program small minimum magnitudes are required. In M3C, on the contrary, the relation is not rejected just like that, since figure 2.13 shows that the choice on minimum magnitude barely has any effect for magnitudes below $M_{min} = 4.0$. A larger minimum magnitude can therefore be used than in EQRISK. Since the M3C program is already tested and debugged, it is assumed that this relation does not give unrealistic results for minimum magnitudes larger than 3.5.

For the relation of Berge-Thierry et al. (2003) the choice of minimum magnitude has a much larger influence: even the curves of $M_{min} = 2.5$ and $M_{min} = 3.0$ are fairly different. This phenomenon can be explained by the way the ground motion prediction equations are being extrapolated to small magnitudes. From figure 2.14 it is clear that the relations of Ambraseys (1995) and Berge-Thierry et al.

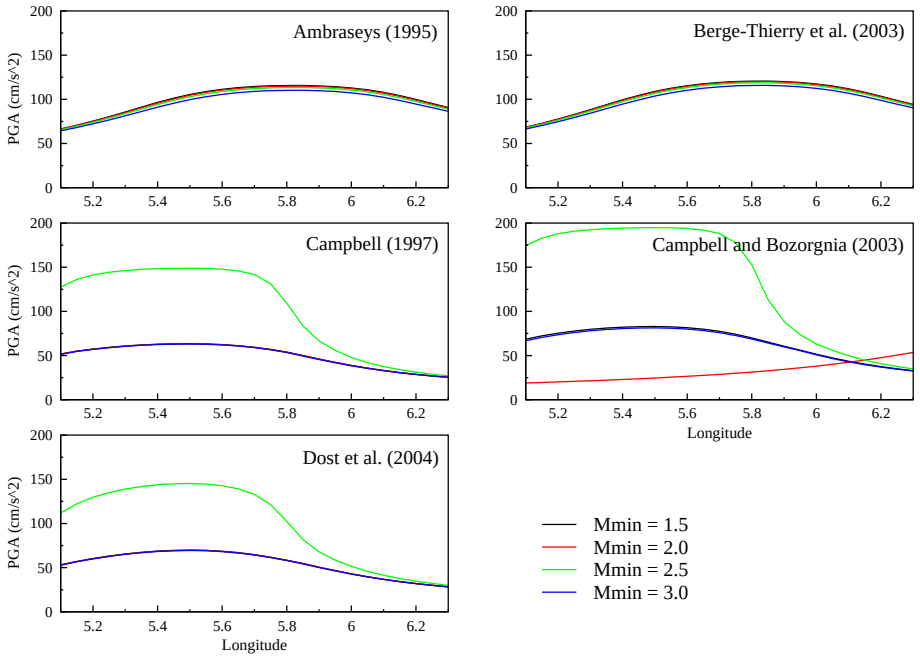

Figure 2.12: Section through Roer Valley Graben in EQRISK, using different minimum magnitudes and ground motion prediction equations.

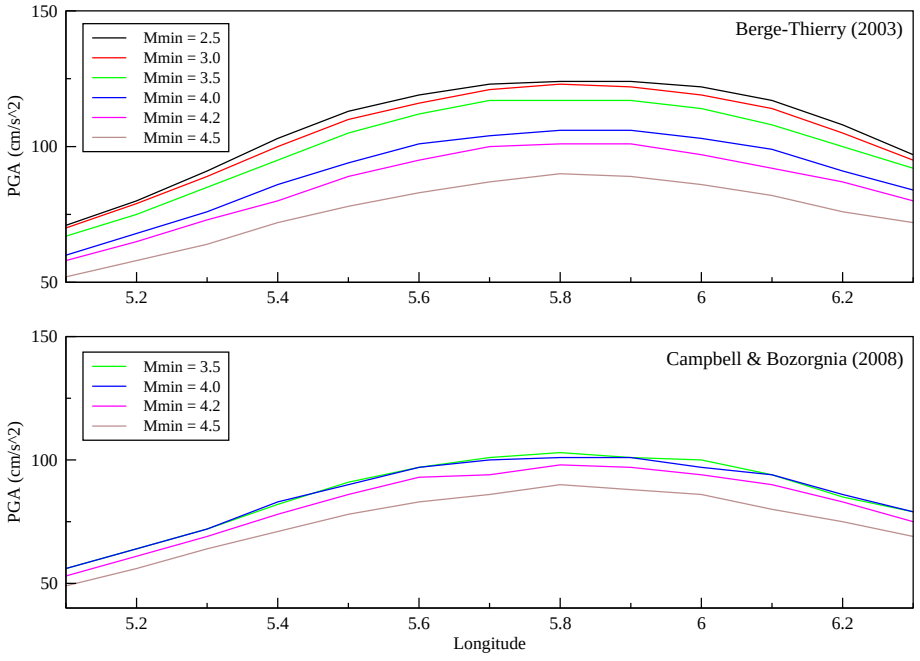

Figure 2.13: Section through Roer Valley Graben in M3C, using different minimum magnitudes and ground motion prediction equations.

(2003) predict much larger peak ground accelerations for small magnitudes than for example Campbell and Bozorgnia (2008). The problem of extrapolation to minimum magnitude has been little addressed in literature. Despite the fact that small magnitude events have barely caused damage in the past, the high accelerations predicted by Berge-Thierry et al. (2003) are not necessarily unrealistic. Musson (written communications) states that small earthquakes do produce significant accelerations, but seismic waves that are generated do not contain frequencies that cause damage to engineering structures. However, Dost et al. (2004) found that most existing ground motion prediction equations overestimate measured peak accelerations for small magnitudes ($M_L < 3.0$) in the Netherlands. For larger magnitudes ($3.0 < M_L < 5.0$), Campbell (1997) predicts the measurements of the Netherlands well. In figure 2.14 Campbell and Bozorgnia (2008) approximates the relation of Dost et al. (2004) (which is the only ground motion prediction equation based on small event data from the Netherlands) the best for small magnitudes. It is also very similar to the relation of Campbell (1997). Therefore, the decision was made to use this ground motion prediction equation for the final seismic hazard map.

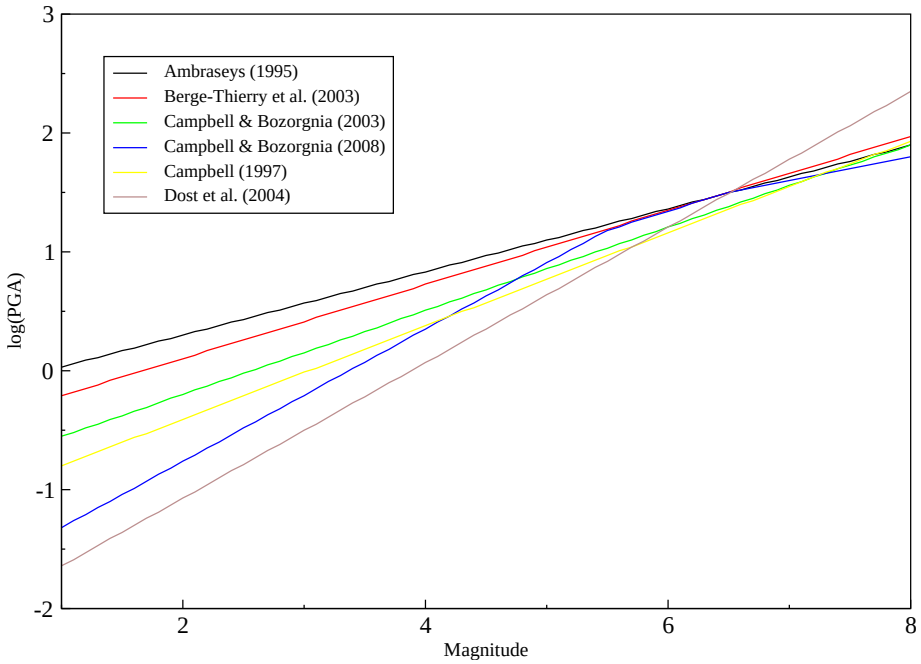

Figure 2.14: Ground motion prediction equations for fixed epicentral distance ($R_e = 100km$) and varying magnitude.

It is very remarkable that the strong influence of minimum magnitude for the Berge-Thierry et al. (2003) relationship in the M3C program is barely visible in EQRISK. This does explain why in figure 2.7 the results of M3C are significantly larger than those of M3C. The fact that in figure 2.9 the hazard is lower in the images of M3C than in those of EQRISK is because in EQRISK much lower magnitudes were used. This phenomenon enhances the suspicion that EQRISK is not suitable for low-seismicity areas. It is therefore decided not to use this program for the final seismic hazard map.

One might expect that for shallower events the impact of the minimum mag-

nitude increases. For several ground motion prediction equations it was shown that (see figure 2.15 for Campbell and Bozorgnia (2008)), when there is a significant difference in PGA for different minimum magnitudes, the difference is larger for shallower events. On the other hand, the magnitude below which the minimum magnitude has no impact (if there is one) remains unchanged for shallower events.

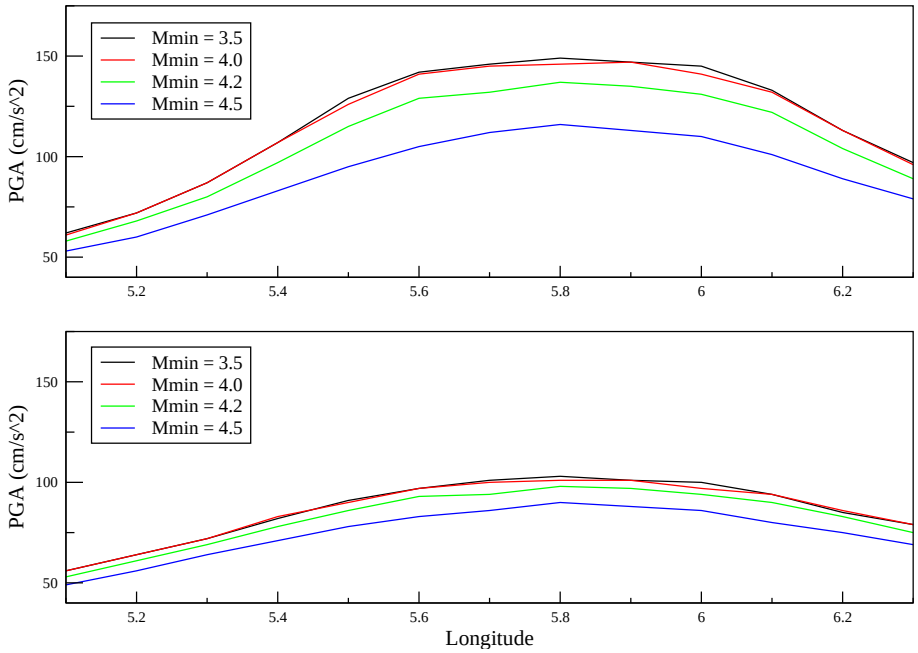

Figure 2.15: Peak Ground Acceleration for different minimum magnitude values using the ground motion prediction equation presented by Campbell and Bozorgnia (2008). The upper part shows the results for a focal depth of 5 km, whereas for the lower part a focal depth of 15 km was used.

2.5.4 Maximum magnitude

Unlike the minimum magnitude, the impact of the choice on maximum magnitude on PGA hazard estimates can be relatively small for moderate seismic regions (Beauval, 2003). From the dataset a maximum magnitude of 6.2 ± 0.2 was found when working in terms of moment magnitude (M_W), which is below a magnitude of 7 approximately equal to the surface wave magnitude (M_S). For local magnitude (M_L) a maximum magnitude of 6.3 ± 0.2 was found. Tests have shown (see figures 2.16 and 2.17) that when the maximum magnitude is increased, the hazard slightly increases, which is not a surprising result. This trend was visible for several different ground motion prediction equations, which suggests that the impact of maximum magnitude does not depend on the choice of attenuation relation. Note that, compared to the effect of the choice of minimum magnitude, the differences are relatively small. This is because the probability of occurrence of a large magnitude is much smaller than for small magnitudes. The maximum magnitudes for source zones that contain large events are chosen to be $M_S = 6.2 \pm 0.2$ and the zones with smaller earthquakes have a maximum magnitude that is half a magnitude unit larger than the largest event ever recorded in the zone. Since the impact of changing the maximum magnitude is not very large, these choices are assumed

to be reasonable.

In the M3C program, the standard deviation on maximum magnitude can be given as input. Figure 2.18 shows a section of the estimated PGA for different values of standard deviation for the maximum magnitude in the Central Roer Valley Graben zone. The standard deviation on maximum magnitude is assumed to be reasonable between 0.05 and 1.0. From the figure the conclusion can be drawn that the choice on variability does not have a significant effect on the hazard estimate. Therefore, it is appropriate to use an uncertainty value of 0.2 for each zone for the final results.

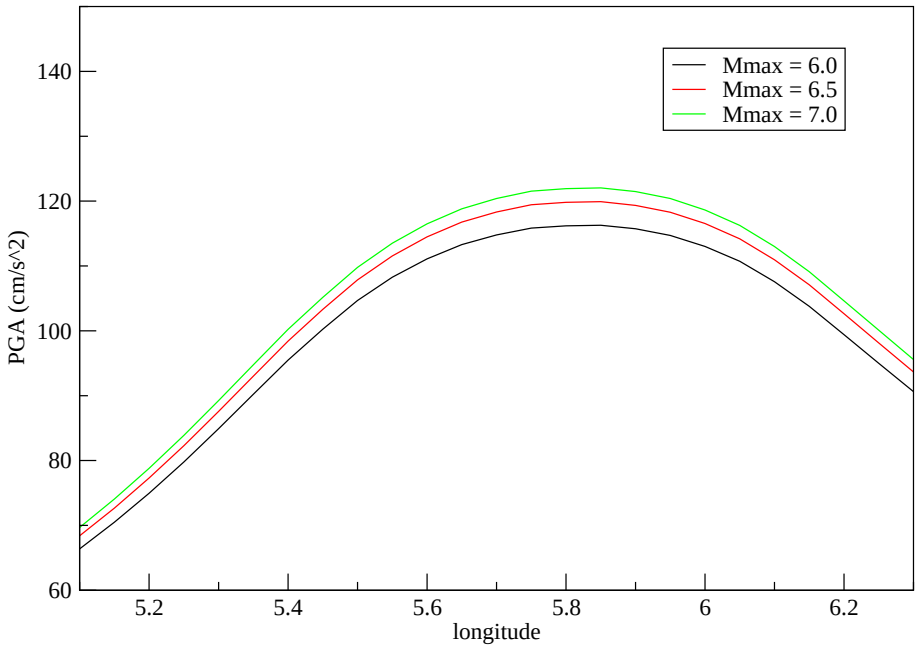

Figure 2.16: Effect of varying maximum magnitude in EQRISK (using relation of Berge-Thierry et al. (2003)).

2.5.5 Seismicity parameters

The seismicity parameters are determined from the earthquake catalogue of the Netherlands and surrounding countries. For moment magnitude the values for A (intercept of the curve of the sum of all zones) and B are found to be 2.87 ± 0.22 and 0.90 ± 0.04, respectively.

In order to decide whether the variabilities on the seismicity parameters are appropriate, different values for these are given as input in the M3C program. Figures 2.19 and 2.20 show sections of the estimated PGA for different values of standard deviation for the A and B values in the Central Roer Valley Graben zone. The standard deviation is assumed to be reasonable between 0.05 and 0.5 for the A value and between 0.005 and 0.1 for the B value. From the figures one can conclude that the choice on variability for the activity rate (A), as well as for the B value, does not have a significant effect on the hazard estimate. Therefore, values of respectively 0.22 and 0.04 will be used for all zones in further experiments.

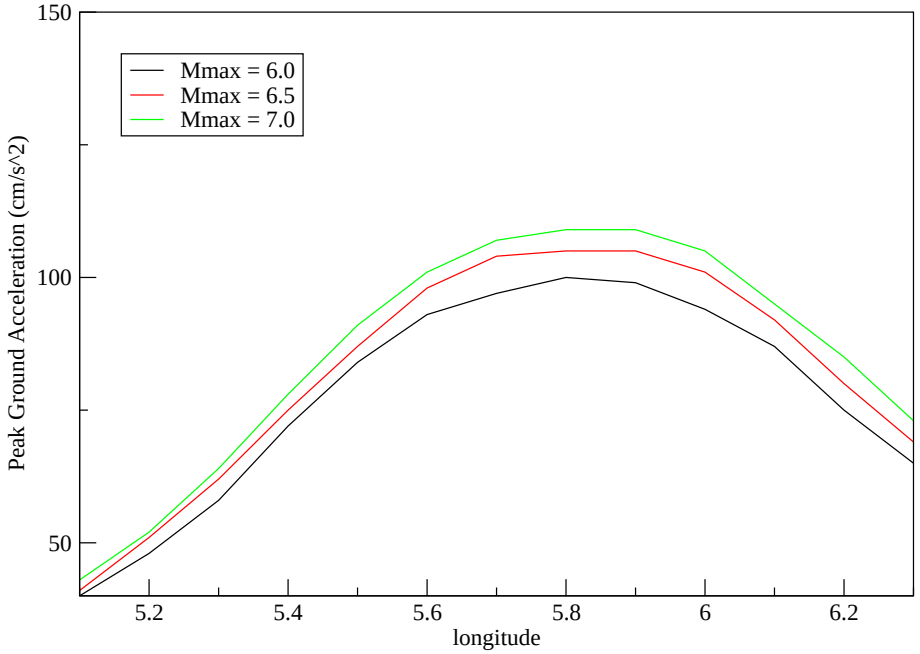

Figure 2.17: Effect of varying maximum magnitude in M3C (using relation of Berge-Thierry et al. (2003)).

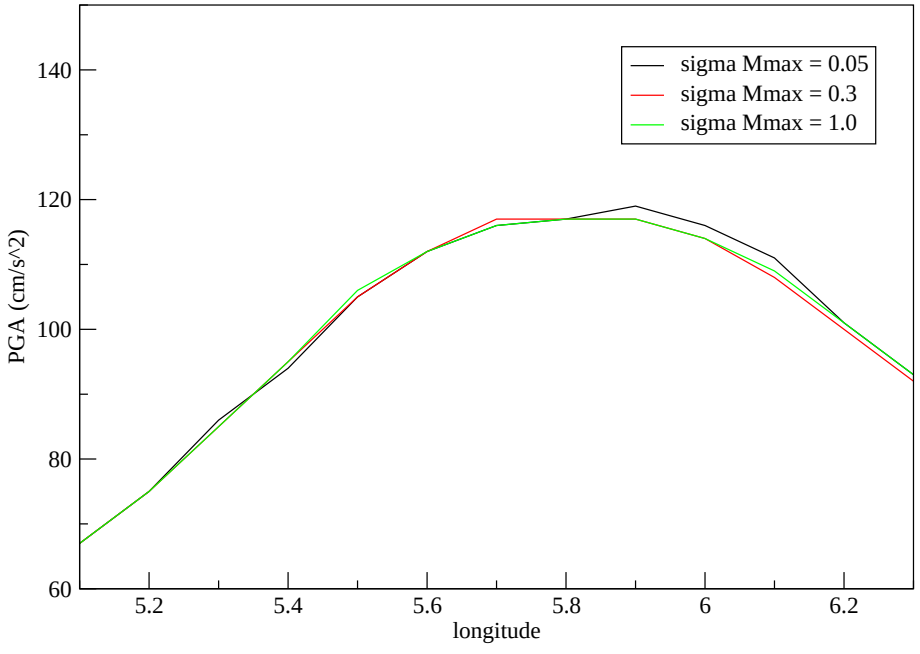

Figure 2.18: Estimation of PGA for different values of variability on Mmax (using relation of Berge-Thierry et al. (2003)).

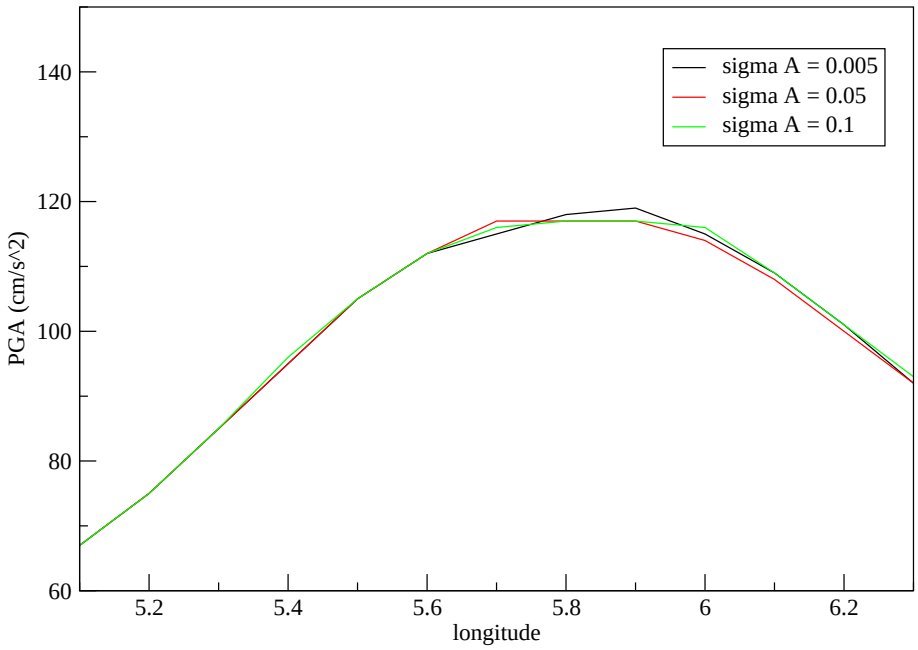

Figure 2.19: Estimation of PGA for different values of variability on A (using relation of Berge-Thierry et al. (2003)).

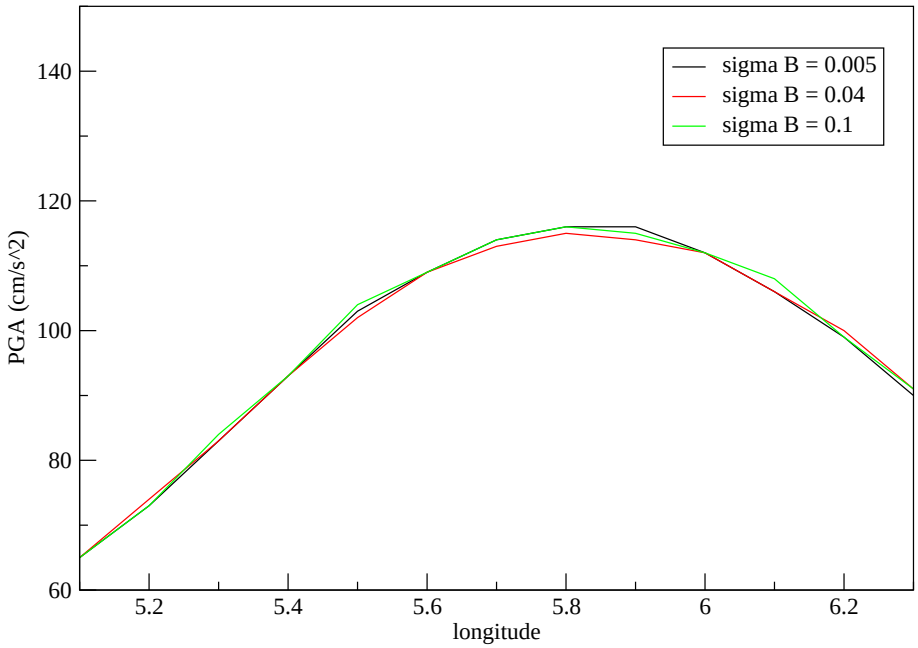

Figure 2.20: Estimation of PGA for different values of variability on B (using relation of Berge-Thierry et al. (2003)).

2.5.6 Source zone definition

Source zones are based on geological, geophysical and seismological characteristics. Very often those features do not agree and it is difficult to make decisions on how to define zone boundaries. A good example for this, which was given earlier, is the Belgian Shear Zone. If zone boundaries are based on seismicity data, the zone will be defined as shown in figure 2.6. However, it would make more sense in geological respect to shift the northern boundary to the north, so it covers the entire Brabant Massif (see figure 2.22). In that case, seismicity will be spread out to the north, for which there is no evidence.

Another subject for debate is the zone that contains the city of Verviers (HOVE). All events recorded in that region had a magnitude smaller than 4.1, except for the large historical earthquake near Verviers, which had a magnitude of 6. Considering this event with the same rate as the smaller events implies that magnitudes between 4.1 and 6 are expected to occur more often than the data base suggests. On the contrary, it would be wrong not to take the Verviers earthquake into account, since there is clear evidence that earthquakes of that size can occur. An alternative would be to define two (geographically equal) zones, one of which contains the small earthquakes, whereas the other contains only large earthquakes occurring at a small rate. However, determining the seismicity parameters by use of a regression technique would be impossible, since only one data point is available. One would therefore have to estimate the A and B values, which would imply a large uncertainty anyhow. For these reasons it was decided to use one zone, taking both the large and small events into account and assuming that magnitudes between 4.1 and 6 can occur.

The same holds for the North Sea zone. Due to the large source-to-receiver distance, small earthquakes at sea are not recorded and only a few large historical events have been reported in the Middle Ages. Location and magnitude for these events are not well determined and, due to the small amount of data, it is very difficult to define the zone boundaries and coefficients of the recurrence relation.

Obviously, (epistemic) uncertainty on source zone definition is very high. More research for the exact location and characteristics of faults would probably enable one to improve the zonation model. However, this would be a difficult and expensive job and in moderately active regions, such as the Netherlands, little research has been done on such topics.

As a consequence, definition of source zones remains subjective and it is important for the hazard analyst to bear in mind what is the impact of the source zonation on the hazard estimates. In order to show this sensitivity, seismic hazard is estimated for two different zonation models, shown in figures 2.21 and 2.22. All other parameters were kept the same.

Figures 2.23 and 2.24 show the results of this test. The images are very similar; only in the northwestern part of Belgium the hazard is slightly higher. This is a consequence of the fact that events are expected to occur in that area in figure 2.22, whereas it is not in figure 2.21. Although not visible due to the presence of the Hainaut zone, the hazard has probably decreased in this part of the area, since the seismicity rate is spread out over a larger area.

However, the peak ground accelerations are still very low and the increase in hazard is therefore considered to be insignificant. The peak ground acceleration value that is interesting for the engineers (0.1 g) will certainly not be exceeded in this area. For the North Sea zone (NSEA) similar results were found. For the

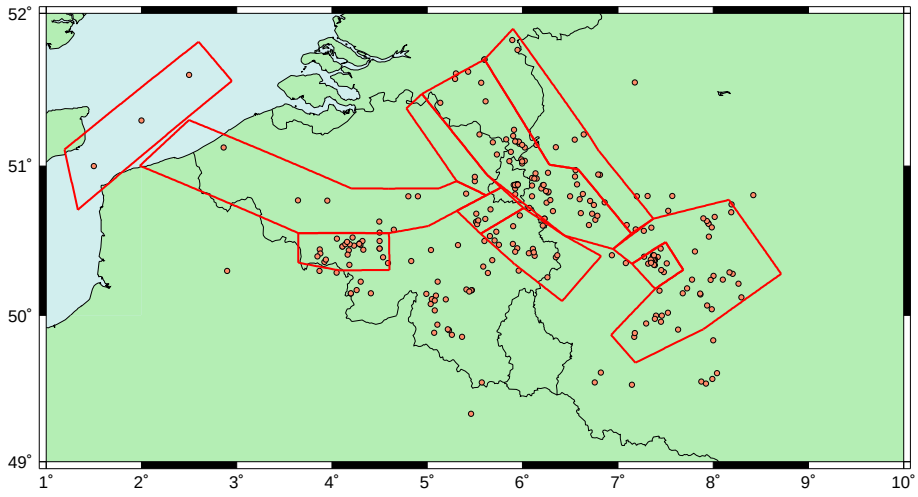

Figure 2.21: Source zonation as used for this study.

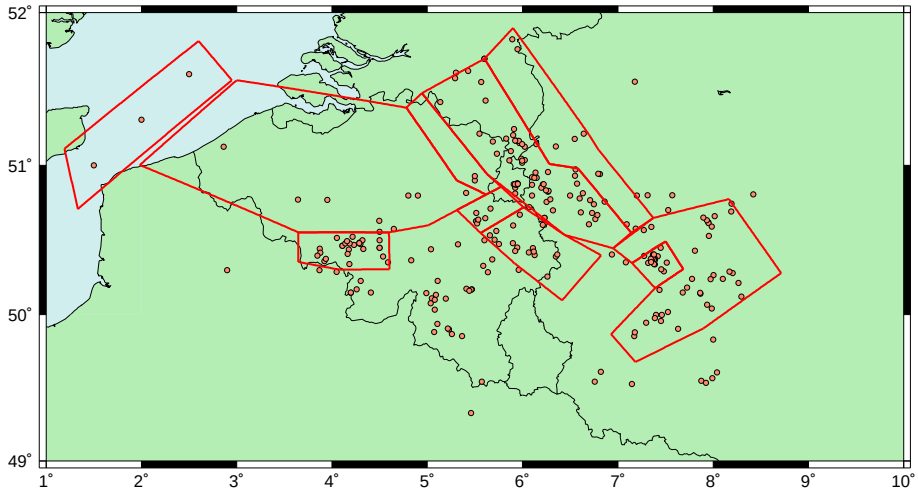

Figure 2.22: Source zonation with alternative for Belgian Brabant Massif Zone (BBMZ).

moment, it is therefore not relevant to investigate these source zone definitions in more detail.

For zones that have higher seismic activity and a larger maximum magnitude than the Belgian Brabant Massif Zone, changing the zonation causes significant differences in peak ground accelerations. For example, if the zones east (RVGE) and west (RVGW) of the central Roer Valley would be included in the Central Roer Valley Graben (RVGC) zone, the area for which significant peak ground accelerations are expected would be much larger than if the three zones would be defined as shown in figure 2.21. The result of combining these three zones (3, 4 and 10) into one zone is shown in figure 2.25. Although peak ground accelerations in the central part of the zone are smaller than in the default model, due to a relatively lower rate of occurrence of events, in the surrounding areas much higher accelerations are expected. This is probably a consequence of the fact that a larger maximum magnitude is assumed for these zones than was done in the zonation model as shown in figure 2.23. There is no consensus about which source zone definition is the best. However, it is decided that the boundaries as defined in figure 2.23 will be used in this study, since they are based on many data, compared to other zones, and it makes sense that large earthquakes only occur along the Feldbiss Fault and the Peel Boundary Fault and not along the surrounding smaller faults.

Although discussion about this topic is still possible, the zonation as defined in this study is assumed to be satisfactory for a preliminary seismic hazard map. More research is required in order to get more certainty about the zonation, but this is beyond the scope of this thesis. Nevertheless, it is important to keep in mind what impact a change in source zonation could have.

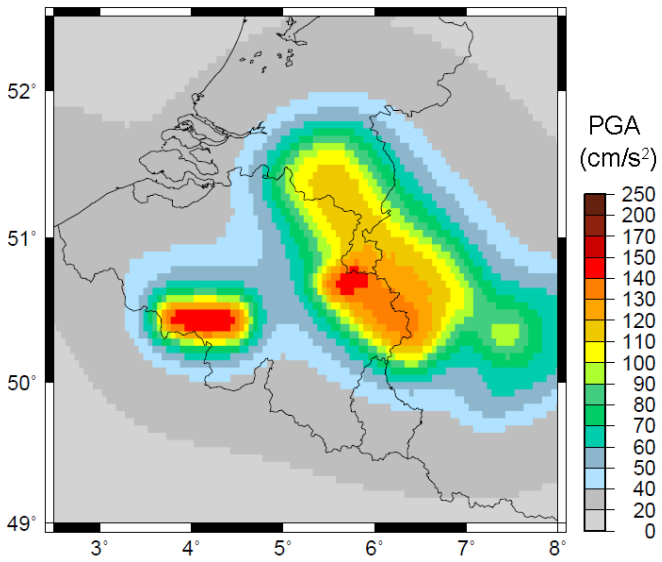

Figure 2.23: Peak Ground Acceleration with 10% probability of exceedence during 50 years (475-year return period) for zonation as shown in figure 2.21.

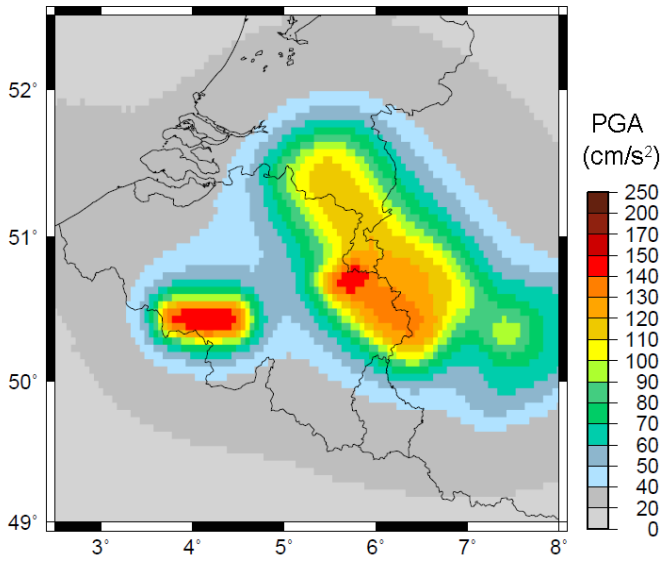

Figure 2.24: Peak Ground Acceleration with 10% probability of exceedence during 50 years (475-year return period) for zonation as shown in figure 2.22.

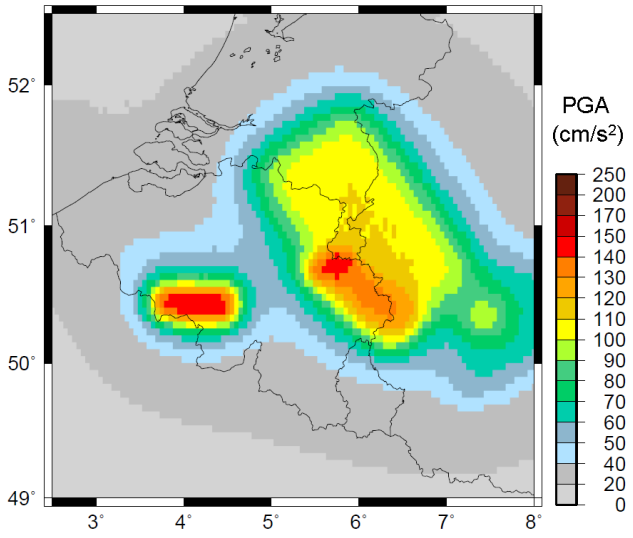

Figure 2.25: Peak Ground Acceleration with 10% probability of exceedence during 50 years (475-year return period) for source zonation in which zone 3, 4 and 10 are combined into one zone.

Chapter 3

Results

The input parameters that were used for the final seismic hazard map are given in table 3.1. The sum of the rates (*i.e.* $N(M \geq 2.5)$), when extrapolated to zero magnitude, equals the A value of 2.87, which was determined in section 2.2. In the M3C program values of 0.22, 0.04 and 0.2, are given for the uncertainties of all rates A, B value, and maximum magnitudes, respectively. In M3C, the ground motion prediction equation presented by Campbell and Bozorgnia (2008) was used and the zonation as given in figure 2.6. Since the ground motion prediction relations of Campbell (1997) and Campbell and Bozorgnia (2003) cannot be used in EQRISK, the relation of Berge-Thierry et al. (2003) was chosen.

Table 3.1: Input parameters for the final seismic hazard map

Zone	Focal depth (km)	M_{min} (EQRISK)	M_{min} (M3C)	M_{max}	N($M \geq 2.5$)	B
1: NEUB	10	1.2	3.5	4.5	0.48	0.90
2: GERM	15	1.0	3.5	4.0	0.85	0.90
3: RVGC	15	2.1	3.5	6.2	1.33	0.90
4: RVGW	10	1.2	3.5	4.5	0.06	0.90
5: LUIK	5	1.6	3.5	5.2	0.13	0.90
6: HOVE	10	2.1	3.5	6.2	0.45	0.90
7: BBMZ	15	1.9	3.5	5.8	0.10	0.90
8: HAIN	5	1.5	3.5	5.0	0.46	0.90
9: NSEA	15	2.1	3.5	6.2	0.07	0.90
10: RVGE	15	1.0	3.5	4.0	0.22	0.90

First, the final seismic hazard map will be presented and discussed. In chapter 4, the results will be compared to the hazard maps that were developed for Belgium (Leynaud et al., 2000) and Germany (Grünthal et al., 2007), as well as to the map presented by De Crook (1996). At the end, recommendations will be given for the improvement of the model.

3.1 Analytical approach

Although the constraints in the program, such as the limited choice on minimum magnitude and the necessity to use a fixed lower magnitude bound (see section 1.2.1,

suggest that the results of EQRISK are less reliable than those of M3C, a seismic hazard map is developed using EQRISK. Input parameters as given in table 3.1 are used. Since the ground motion prediction relations of Campbell (1997), Campbell and Bozorgnia (2003) and Dost et al. (2004) cannot be used in the program, only the relations of Ambraseys (1995) and Berge-Thierry et al. (2003) are left. Both these relations give similar results; the ground motion prediction equation of Berge-Thierry et al. (2003) is used for the final version of the seismic hazard map in EQRISK, which is shown in figure 3.1.

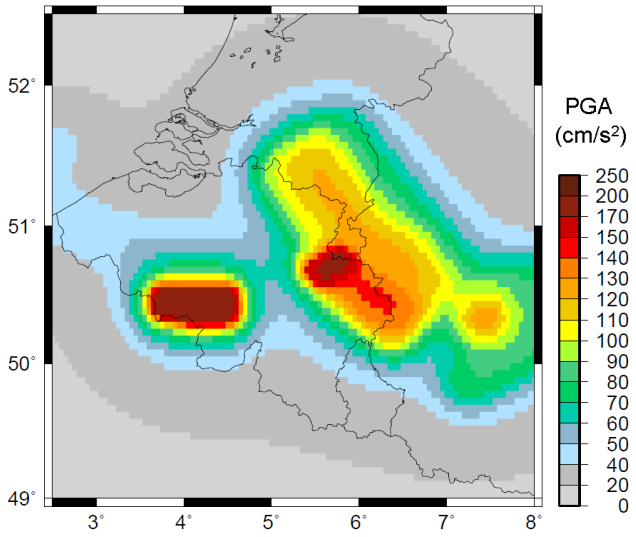

Figure 3.1: Peak Ground Acceleration with 10% probability of exceedence during 50 years (475-year return period) given by EQRISK for the input parameters described in table 3.1. The attenuation law of Berge-Thierry et al. (2003) and zonation as shown in figure 2.6 are used.

Compared to the results of M3C and those of other studies (see next paragraph/chapter), the peak ground acceleration values are approximately 30% higher. Although this is not impossible, it is very unlikely that accelerations of such values will be exceeded in a period of 475 years. Also, due to the restrictions in the program, it is very difficult to decide whether the result is reliable and what causes the unexpected values. This version of the seismic hazard map will therefore not be used as a final result for the Eurocode 8.

3.2 Monte Carlo approach

Using the input parameters as given in table 3.1 and the ground motion prediction equation of Campbell and Bozorgnia (2008), the resulting seismic hazard map looks as shown in figure 3.2. It is clear that seismic hazard is particularly high for zones in which shallow events occur. Also, the high rate of occurrence in for example the Central part of the Roer Valley causes relatively large peak ground accelerations.

Also remarkable is the fact that the boundaries of the source zones are very clear. This suggests that seismic hazard is mainly high for small source-to-site dis-

tances, whereas at larger distances peak ground acceleration decreases very fast. This was mentioned earlier in section 2.5.

According to this version of the seismic hazard map, the rules of Eurocode 8 should be applied for engineering structures only in Limburg and the eastern part of Noord-Brabant (not considering areas outside the Netherlands). For this map, however, the magnitude-frequency relation is abruptly truncated at the maximum magnitude. The M3C program offers the opportunity to smoothly taper-off the relation, which is more realistic. If this option is active in each zone, the resulting seismic hazard map looks as shown in figure 3.3. An overall decrease of seismic hazard is visible, but the effect is particularly large in zones that contain shallow events. This is to be expected, since large events at shallow depth cause larger peak ground accelerations compared to deep events and the effect of reducing the rate of these events will therefore be larger as well.

Since the M3C program has many possibilities and the source code is not available, it is difficult to control each input parameter. Many options, such as 'curve max value', limits to the uncertainties and 'epicentral scatter' are determined as good as possible (or turned off, if possible), but the amount of parameters that should be given is too large to investigate the sensitivity of the hazard estimate to each parameter separately. Some small tests were performed considering these parameters (which are not useful for this study) and it seemed that they did not have significant impact, but more research is required to confirm this. However, the M3C program is still considered to give more realistic results than EQRISK, mainly because M3C was developed particularly for low-seismicity areas and has been tested already. The version of the seismic hazard map shown in figure 3.3 is therefore considered to be the most realistic one.

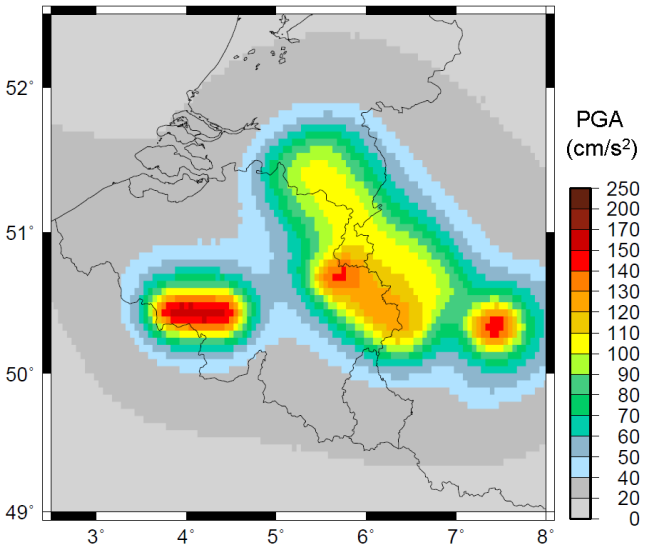

Figure 3.2: Peak Ground Acceleration with 10% probability of exceedence during 50 years (475-year return period) given by M3C for the input parameters described in table 3.1. The attenuation law of Campbell and Bozorgnia (2008) and zonation as shown in figure 2.6 are used.

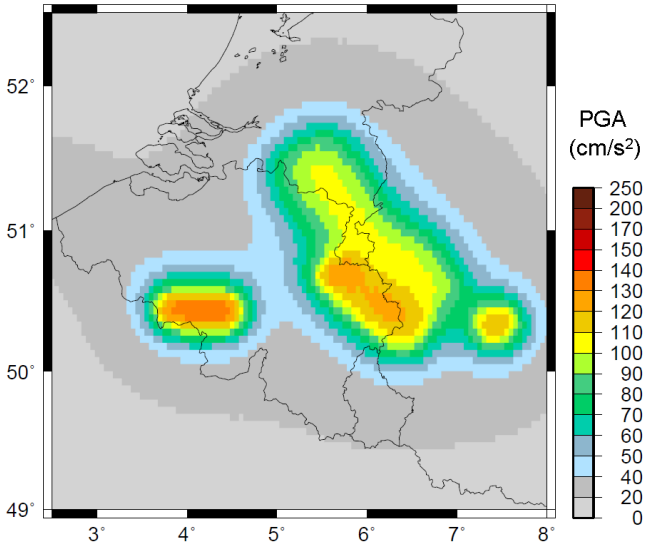

Figure 3.3: Peak Ground Acceleration with 10% probability of exceedence during 50 years (475-year return period) given by M3C for the input parameters described in table 3.1. The attenuation law of Campbell and Bozorgnia (2008) and zonation as shown in figure 2.6 are used. The magnitude-frequency relation is tapered-off smoothly.

Chapter 4

Discussion and Conclusions

From the tests, which are discussed in section 2.5, it can be concluded that the seismic hazard estimate mainly depends on the definition of the source zonation model and the choice on ground motion prediction equation. The latter includes the impact of minimum magnitude and focal depth, which causes the large sensitivity to the choice on ground motion prediction equation.

The final seismic hazard map presented in figure 3.3 should not be interpreted as the only possible version. Since the model is based on a probabilistic model, rather than on factual knowledge, it is impossible to present a map that shows the exact locations where the limiting acceleration of 0.1 g will be certainly exceeded and where it will not. For example, when a grid cell has a peak ground acceleration value between 90 cm/s^2 and 100 cm/s^2, it does not necessarily mean that the limiting value will never be exceeded. For regions where the expected peak ground acceleration is smaller than 100 cm/s^2, but still inside the uncertainty range (which is estimated to be of the order of 30 cm/s^2 from the tests in section 2.5), it might be recommended to take the Eurocode 8 rules into account, even when the hazard map suggests that it is not necessary. This, however, is up to the user to decide. On the contrary, there are also regions on the map where accelerations are expected that are much smaller than 100 cm/s^2 and fall outside the uncertainty range. For these regions it is very unlikely that the limiting value will ever be reached. Of course the model can be improved, but it will be very difficult to reduce the uncertainty (see section 4.2).

4.1 Comparison to other seismic hazard models

What might help in testing whether the model makes sense is comparison to other independent models. The seismic hazard maps developed by Leynaud et al. (2000) (Belgium) and Meskouris (2005) (Germany), which is used for the German national annex of the Eurocode 8, are shown in figures 4.1 and 4.2, respectively. A seismic hazard map for Germany, Austria and Switzerland was developed by Helmholtz Centre Potsdam - GFZ German Research Centre for Geosciences (2008), which is very similar to that shown in figure 4.2. The only differences are that the map extends further south and that intensity values below 6 are shown. Since this does not contribute to a better comparison, this map is not discussed in further detail.

Figure 4.1 and the hazard map presented in this study look very similar. The largest hazard occurs in the Hainaut and Liège zones. This similarity might be caused by the fact that similar zonations were applied in the model. On the

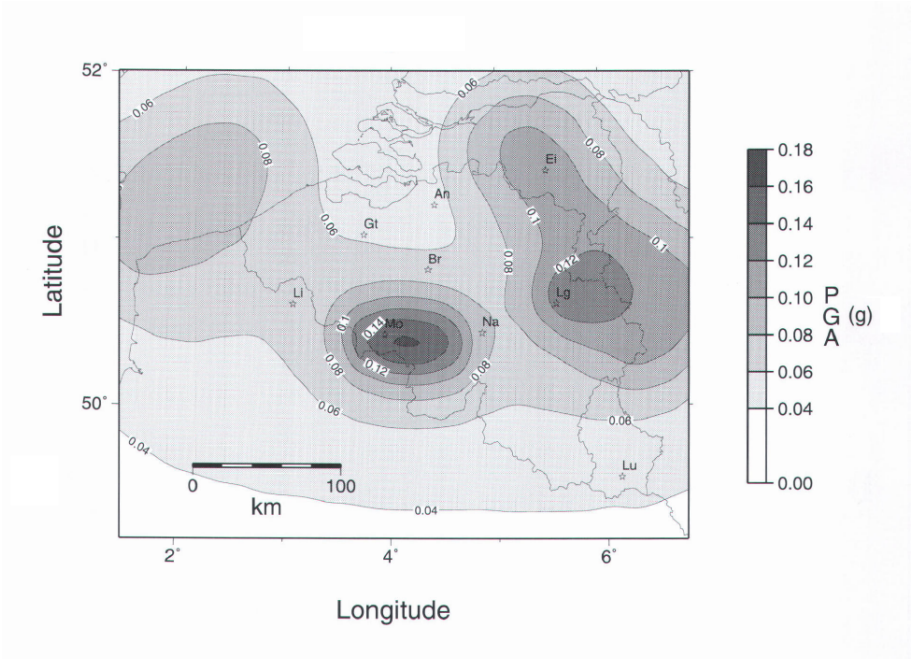

Figure 4.1: Peak Ground Acceleration with 10% probability of exceedence during 50 years (475-year return period) for Belgium (Leynaud et al., 2000).

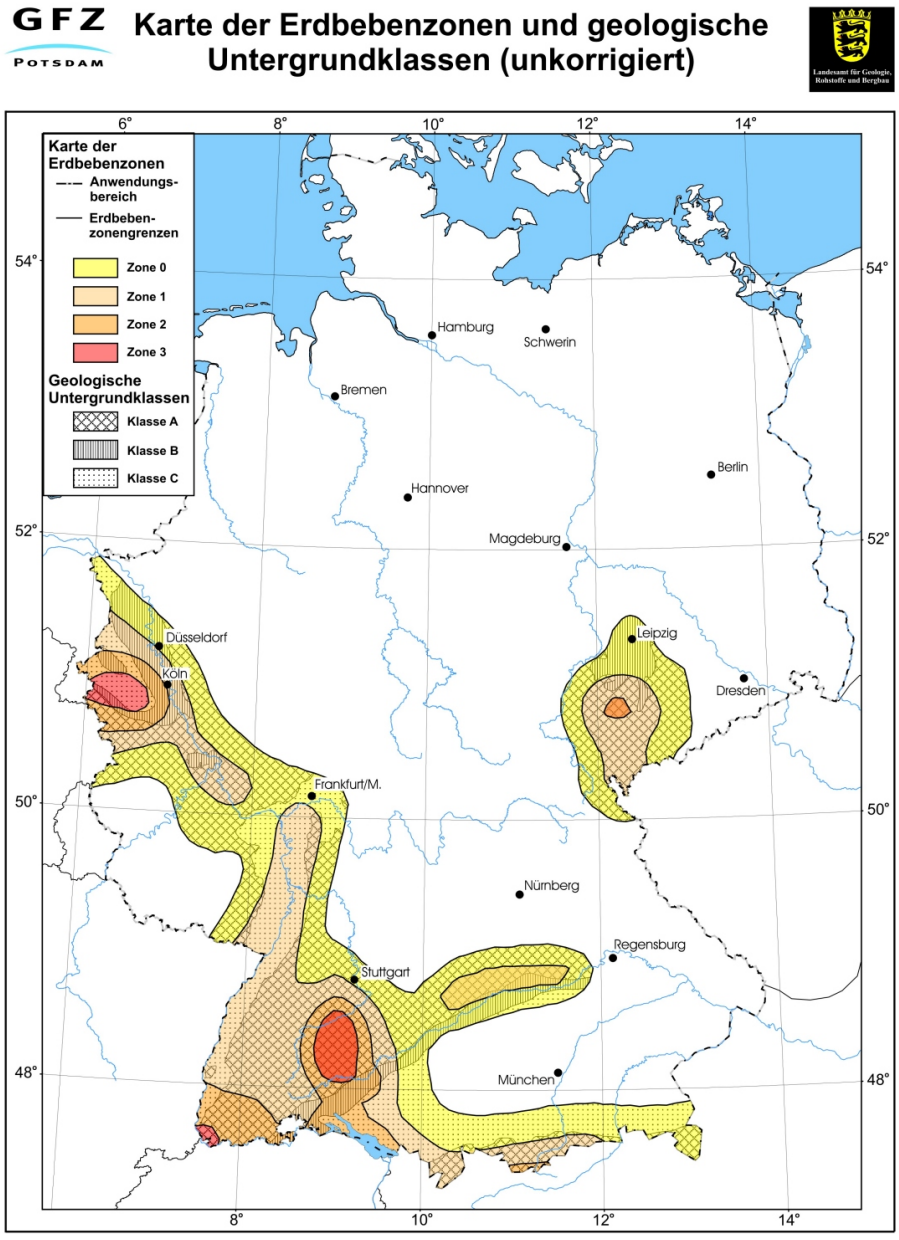

Figure 4.2: Peak Ground Acceleration with 10% probability of exceedence during 50 years (475-year return period) for Germany (Meskouris, 2005), based on intensities. Zone 0: $I = 6$ ($\sim$ 50 cm/s^2), Zone 1: $I = 6.5$, Zone 2: $I = 7$ ($\sim$ 100 cm/s^2), Zone 3: $I = 7.5$.

other hand, Leynaud et al. (2000) uses the ground motion prediction equation of Ambraseys (1995), whereas in this study a rather different relation is used (Campbell and Bozorgnia, 2008), which is expected to give different results. Also, the approaches used are not similar, which suggests that the seismic hazard models are stable. A remarkable difference between the two models is the hazard in the western part of the area; the model of Leynaud et al. (2000) predicts significantly larger accelerations than the model in this study. This is probably a consequence of the small amount of data available, which results in large differences in the estimation of seismicity parameters, especially the rate of occurrence, for this zone. A possible way to check this would be to use the values of Leynaud et al. (2000) in the model of this study.

The results of Meskouris (2005) are more difficult to compare to the hazard map of this study, since the seismic hazard assessment for Germany was based on intensities, rather than peak ground accelerations. Conversion of intensities to PGA introduces a significant uncertainty. Another problem is that the model of Meskouris (2005) is restricted to the German borders, which makes it even more difficult to compare the figures. The values that are predicted in the Roer Valley are slightly larger than 100 cm/s^2, which seems to agree fairly well with the accelerations found in this study. In the Neuwied area, however, predicted accelerations are much smaller in the German model, than they are in this study. This is most probably due to the different zonations used.

Another model that has been proposed for Germany and is based on peak ground accelerations is shown in figure 4.3. Again, the model of Grünthal et al. (2007) is restricted to the German borders, which makes it difficult to compare it with the model presented in this study. Also, a slightly different return period 0f 500 years is used. The acceleration values predicted by the model of Grünthal et al. (2007) are approximately 100 cm/s^2 for the Roer Valley area and 60 cm/s^2 for the Neuwied Basin area. Again, the values predicted for the Roer Valley seem to agree fairly well, whereas in the Neuwied area predicted accelerations are much smaller in the German model. This is probably a consequence of the fact that in Grünthal et al. (2007) the Neuwied basin is not a distinct zone. It is not clear whether the zonation used by Grünthal et al. (2007) makes more sense. Regardless of which one of the models is used, the impact in the Netherlands can be neglected anyway. The certainty of the zonation in that area is therefore not of great importance for this study.

Figure 4.4 shows the seismic hazard map as presented in the latest study for the Netherlands (De Crook, 1996). This seismic hazard model is very different from the model presented in this study. Besides the fact that predicted peak ground accelerations are smaller than in figure 3.3, the hazard extends much further to the north. Probably, this is due to the different zonation model used. De Crook (1996) based his model on intensities, rather than peak ground acceleration, which introduces an additional uncertainty in the comparison. Also, for the study of De Crook (1996) less data were available than for this study.

A seismic hazard map for Europe on the whole is presented by Jimenez et al. (2003). Although the source zonation for the area of interest is not as detailed as in this study, similar peak accelerations are found.

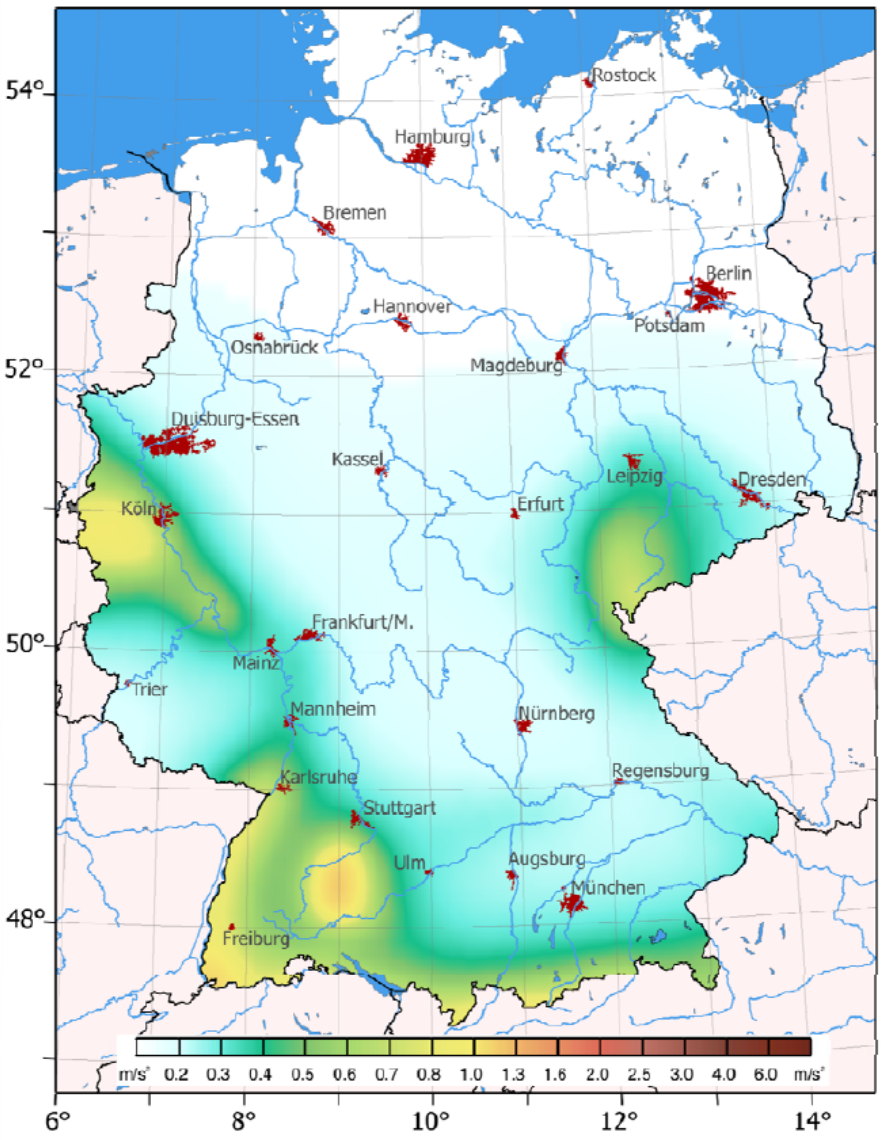

Figure 4.3: Peak Ground Acceleration with 18% probability of exceedence during 100 years (500-year return period) for Germany (Grünthal et al., 2007). Note that the return period is slightly different from that used in this study.

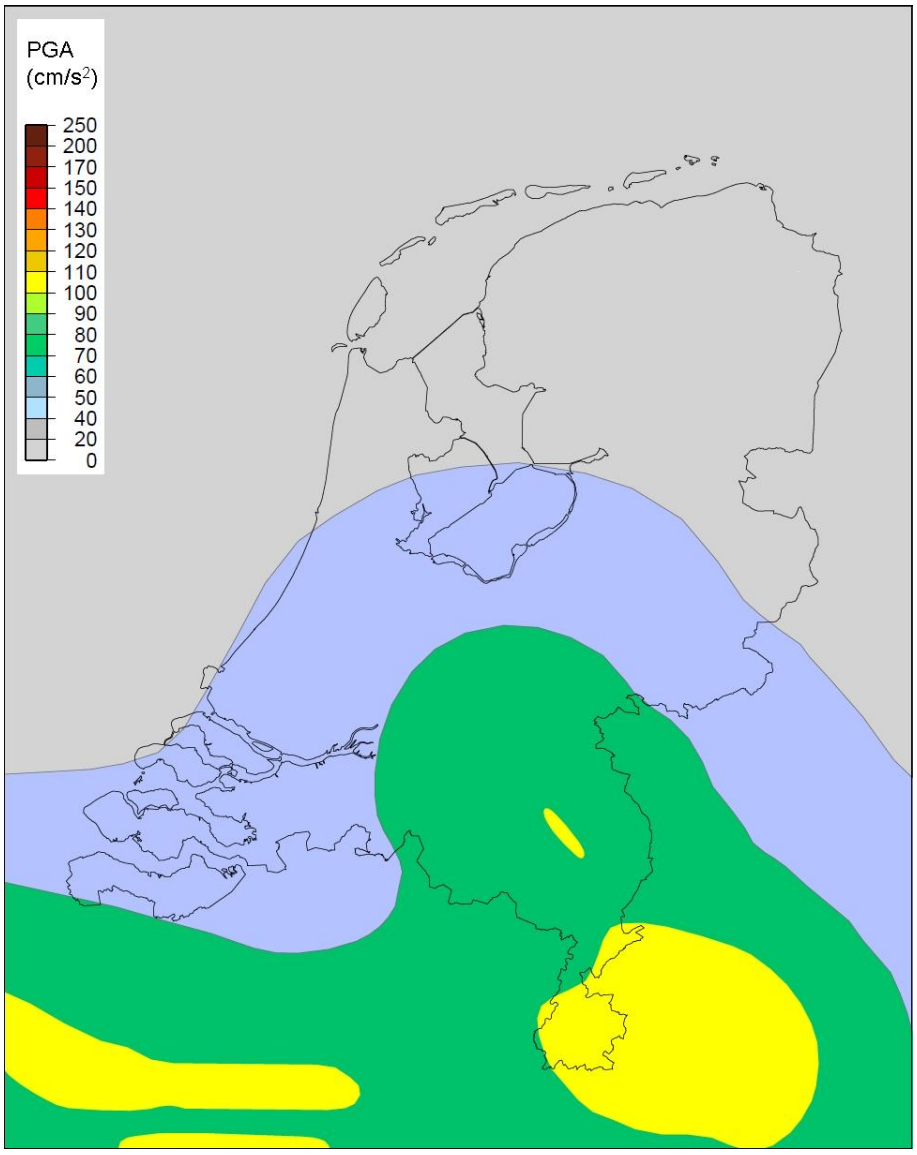

Figure 4.4: Peak Ground Acceleration with 10% probability of exceedence during 50 years (475-year return period) for the Netherlands (De Crook, 1996).

4.2 Recommendations for the improvement of the model

During this research different methodologies have been investigated and a preliminary version of a seismic hazard map for the Netherlands is developed. Also, a first impression is given of the sensitivity of the hazard estimate to different parameters. The next step would be to quantify the uncertainty of the hazard estimate and include this in the resulting seismic hazard map.

As stated earlier, the choice of ground motion prediction equation has a large influence on the seismic hazard estimate. Unfortunately, no relations are available that are particularly based on data from the area of interest. Dost et al. (2004) used data from the Netherlands, but these were mainly from very shallow, small-magnitude events, which are not representative for large parts of the area, and the amount was insufficient to develop a relation that is reliable for the considered magnitude range. The ground motion prediction equation that was used for the final hazard map (and some other relations (Dost et al., 2004; Campbell, 1997; Campbell and Bozorgnia, 2003)) cause problems when a minimum magnitude smaller than 3.2 is used. This problem remains unsolved for this study. It is strongly recommended to investigate this in further research.

Also, more attention could be paid to the relation presented by Atkinson and Boore (2006). Since it has been developed quite recently, it is not clear yet, whether this model is realistic. If so, this relation might certainly be useful for the Netherlands, since it is developed for intra-plate earthquakes and considers relatively small magnitudes.

Furthermore, it would be very useful if a ground motion prediction equation would be developed for a magnitude range that considers magnitudes up to approximately 6.5, but also requires no extrapolation to smaller magnitudes. For example, development of a special ground motion prediction equation for north-western Europe (which is, in contrast to the other regional relations, not based on data from active regions such as Italy and Greece) would be very useful. However, this is difficult, due to the small amount of data available. Another useful thing would be to investigate how the extrapolation to small magnitudes should be done. The question is whether the large uncertainty band might be reduced, or such differences in peak ground acceleration can be caused by different fault mechanisms (Dost et al., 2004).

Another point that might contribute to the improvement of the model would be to perform more research on the zonation model. Although some zone boundaries are fairly well known, much more geological and geophysical knowledge is required to define each single zone with a large certainty. Also, more data are required in order to define seismicity parameters and focal depths more properly. However, since the activity is very low in the Netherlands, little new data are available and it will probably remain difficult to achieve better results. Furthermore, it would be useful to investigate the local site conditions in more detail. For this study, soil type is assumed to be similar for all zones. This is clearly not the case in reality and, since local site conditions are thought to be of large influence, refining the model on this point would probably improve the hazard estimate.

Another suggestion to make the hazard map more useful for the Netherlands is to include induced seismicity. At the moment, the seismic hazard map suggests that there is no significant hazard in the Northern part of the Netherlands. Some events from the past have shown that this is not the case and with continuing gas exploration this will not change. A study considering seismic hazard for induced

earthquakes in the northern part of the Netherlands is performed earlier by Eck et al. (2006). Since EQRISK was used and input parameters can be updated, this study needs to be revised (for example using M3C) and included in the seismic hazard map study for tectonic earthquakes. Revision of the input parameters of induced seismicity and making it suitable for the M3C program would take much time and it is therefore not included in this study.

Finally, computer codes could be adapted in such a way that they are better applicible to the area. For EQRISK, this would imply solving the problem of the constraint on magnitude bounds due to the $ANEQ$ term. In order to do this, one has to go deeply into the details of the theory and source code, which is a time-consuming task. For M3C, on the other hand, it would be very useful to get access to the source code, so other ground motion prediction equations can be implemented and required input parameters can be adapted to the model.

Appendix

AUTHOR	GROUND MOTION PREDICTION EQUATION	UNIT	UNCERTAINTY	DATA ORIGIN (AMOUNT)
Berge-Thierry *et al.* (2003)	$\log PSA = 1.576 + 0.3114M - 0.0009334r - \log r$	cm/s^2	$\log\sigma = 0.29$ $\ln\sigma = 0.67$	European Strong Motion Database (965) + America (8)
Ambraseys (1995)	$\log a_h = -1.151 + 0.266M - 0.00022r - 1.024\log r$	g	$\log\sigma = 0.25$ $\ln\sigma = 0.58$	Europe + Middle East (1260)
Ambraseys *et al.* (1996)	$\log a = -1.363 + 0.266M - 0.922\log r$	g	$\log\sigma = 0.25$ $\ln\sigma = 0.58$	Europe + Middle East (422)
Ambraseys *et al.* (2005)	$\log y = 2.488 - 0.142M + (-3.184 + 0.314M)\log r$	m/s^2	$\log\sigma_T = \sqrt{\sigma_1^2 + \sigma_2^2}$ $\sigma_1 = 0.665 - 0.065M$ $\sigma_2 = 0.222 - 0.022M$	Europe + Middle East (595): Seismically active regions
Atkinson and Boore (2006)	$\log PGA = 0.740 + 0.969M - 0.0620M^2 + (-2.44 + 0.147M)\min[\log r;\log 70] + (-2.34 + 0.191M)\max[\log\frac{r}{140};0] + (-0.087 - 0.0829M)\max[\log\frac{10}{r};0] - 6.30\cdot 10^{-4} r$	cm/s^2	$\log\sigma = 0.30$ $\ln\sigma = 0.69$	NE US + SE Canada (1700): Hard-rock sites
Bommer *et al.* (2007)	$\log PGA = -0.0053 + 1.0848M - 0.0835M^2 + (-2.4423 + 0.2081M)\log r$	cm/s^2	$\log\sigma_T = \sqrt{\sigma_1^2 + \sigma_2^2}$ $\sigma_1 = 0.599 - 0.058M$ $\sigma_2 = 0.323 - 0.031M$	Europe + Middle East (997)
Campbell (1997)	$\ln a_h = -3.512 + 0.904M - 1.328\ln\sqrt{r^2 + [0.149e^{0.647M}]^2}$	g	$\begin{cases} 0.55, & a_h < 0.068g \\ 0.173 - 0.14\ln a_h, & 0.068g \le a_h \le 0.21g \\ 0.39, & a_h > 0.21g \end{cases}$	Worldwide (645): Seismically active regions
Campbell and Bozorgnia (2003)	$\ln a_h = -2.896 + 0.812M - 1.318\ln\sqrt{r^2 + [0.187e^{0.616M}]^2}$	g	$\begin{cases} 0.57, & a_h \le 0.07g \\ 0.219 - 0.132\ln a_h, & 0.07g < a_h < 0.25g \\ 0.402, & a_h \ge 0.25g \end{cases}$	Worldwide (1403): Active, shallow crustal regions
Campbell and Bozorgnia (2008)	$\ln\hat{Y} = -0.128 + (-2.118 + 0.17M)\ln\sqrt{r^2 + (5.6)^2} + f_{site} + f_{mag}$ *	g	variable	NGA database (PEER) (1561)
Dost *et al.* (2004)	$\log a_h = -1.41 + 0.57M - 0.00139r - 1.33\log r$	m/s^2	$\log\sigma = 0.33$ $\ln\sigma = 0.76$	The Netherlands, Roswinkel + Voerendaal (~50)

Table: Description of the ground motion prediction equations as used in this study. Note that some relationships use base ten logarithms, whereas others use natural logarithms. Sometimes PGA is given in g and sometimes in cm/s^2; final PGA values are given in cm/s^2 by EQRISK and in g by M3C.

MAGNITUDE TYPE	MAGNITUDE DOMAIN	DEPTH DEPENDENT?	DISTANCE DEFINITION	DISTANCE DOMAIN	LOCAL SITE CONDITIONS	FAULT MECHANISM	REGRESSION TECHNIQUE	COMPUTER CODE	REMARKS
M_S	4 - 7.9	YES	$r = \sqrt{d_e^2 + h^2}$	4 - 330 *km* h < 30 *km*	Alluvium	-	Two-step inversion method	EQRISK + M3C	5% damped, mean component
M_S	2 - 7.3	YES	$r = \sqrt{d_{JB}^2 + h^2}$	M = -1.5-0.025r h < 25 *km*	-	-	Two-stage regression	M3C	maximum component, large location errors for small events, little high-frequency recordings
M_S	4 - 7.9	NO	$r = \sqrt{d_{JB}^2 + h_0^2}$ $h_0 = 3.5$	0 - 200 *km* 2 < h < 30 *km*	Stiff soil	-	Two-state regression	EQRISK + M3C	maximum component
M_W	5 - 7.7	NO	$r = \sqrt{d_{JB}^2 + h_0^2}$ $h_0 = 7.6$	0 - 100 *km*	Stiff soil	Normal	One-stage maximum likelyhood, weighted regression	EQRISK + M3C	5% damped, maximum component
M_W	3.5 - 8	YES	Shortest distance to fault rupture	1 - 1000 *km* 2 < h < 30 *km*	Soil	-	Stochastic finite fault approach	M3C	random component, theoretical model, should not make much difference when applied to mid-continent
M_W	3 - 7.6	NO	$r = \sqrt{d_{JB}^2 + h_0^2}$ $h_0 = 8.0282$	0 - 100 *km*	Stiff soil	Normal	One-stage maximum likelyhood	M3C	5% damped
M_W	4.7 - 8	YES	Shortest distance between recording site and presumed zone of seismogenic rupture on the fault	3 - 60 *km* h < 25 *km*	Alluvium/ Firm Soil	Normal	Unweigted generalized non-linear least-squares	EQRISK	5% damped, mean component
M_W	4.7 - 7.7	YES	Shortest distance between recording site and presumed zone of seismogenic rupture on the fault	3 - 60 *km* h < 25 *km*	Firm soil	Strike-Slip Normal	Generalized non-linear least-squares	EQRISK	5% damped, overprediction at r > 100 *km*
M_W	4.3 - 7.9	YES	Shortest distance between recording site and presumed zone of seismogenic rupture on the fault	0.1 - 199 *km*	Soft soil	Normal	Two-stage least-squares	M3C	5% damped, mean component, data from stable continental region excluded
M_L	2.3 - 3.9	YES	$r = \sqrt{d_e^2 + h^2}$	0 - 5 *km*	-	-	-	EQRISK	5% damped, mean component

* $f_{mag} = \begin{cases} -1.715 + 0.5M, & M \le 5.5 \\ -1.715 + 0.5M - 0.53(M - 5.5), & 5.5 < M \le 6.5 \\ -1.715 + 0.5M - 0.53(M - 5.5) - 0.262(M - 6.5), & M > 6.5 \end{cases}$ $f_{site} = 1.058\ln\left(\frac{270}{865}\right) - 1.186\left\{\ln\left[A + 1.88\left(\frac{270}{865}\right)^{1.18}\right] - \ln(A + 1.88)\right\}$ $A = \ln\hat{Y}$, *with* $f_{site} = -0.34148\ln\left(\frac{1100}{865}\right)$

Bibliography

Ahorner, L. (1983a). Historical seismicity and present-day microearthquake activity of the rhenish massif, central europe. In Fuchs, K., von Gehlen, K., Mälzer, H., Murawski, H., and Semmel, A., editors, *Plateau Uplift; The Rhenish Shield - A Case History.*, pages 198 – 219. Springer-Verlag.

Ahorner, L. (1983b). Seismicity and neotectonic structural activity of the Rhine Graben System in Central Europe. In Ritsema, A. and Gürpinar, A., editors, *Seismicity and seismic risk in the offshore North Sea area*, pages 101 – 111. D. Reidel, Dordrecht.

Ambraseys, N. (1995). The prediction of earthquake peak ground acceleration in Europe. *Earthquake engineering and structural dynamics*, 24: 467 – 490.

Ambraseys, N., Douglas, J., Sarma, S., and Smit, P. (2005). Equations for the estimation of strong ground motions from shallow crustal earthquakes using data from Europe and the Middle East: Horizontal peak ground acceleration and spectral acceleration. *Bulletin of Earthquake Engineering*, 3: 1 – 53.

Ambraseys, N., Simpson, K., and Bommer, J. (1996). Prediction of horizontal response spectra in Europe. *Earthquake engineering and structural dynamics*, 25: 371 – 400.

Atakan, K., Ojeda, A., Camelbeeck, T., and Meghraoui, M. (2001). Seismic hazard analysis results for the Lower Rhine Graben and the importance of paleoseismic data. *Geologie en Mijnbouw*, 80 (3 – 4): 305 – 314.

Atkinson, G. and Boore, D. (2006). Earthquake Ground-Motion Prediction Equations for Eastern North America. *Bulletin of the Seismological Society of America*, 96: 2181 – 2205.

Beauval, C. (2003). *Analyse des incertitudes dans une estimation probabiliste de l'aléa sismique, exemple de la France*. PhD thesis, Université Joseph Fourier - Grenoble I.

Bender, B. and Perkins, D. (1987). SEISRISK III: A computer program for seismic hazard estimation. Bulletin 1772, United States Geological Survey. 24 p.

Berg, M. v. d., Vanneste, K., Dost, B., Lokhorst, A., Eijk, M. v., and Verbeek, K. (2002). Paleoseismic investigations along the Peel boundary fault: geological setting, site selection and trenching results. *Geologie en Mijnbouw*, 81 N. 1: 39 – 60.

Berge-Thierry, C., Cotton, F., and Scotti, O. (2003). New empirical response spectral attenuation laws for moderate European earthquakes. *Journal of Earthquake Engineering*, 7 N. 2: 193 – 222.

Bommer, J., Stafford, P., Alarcón, J., and Akkar, S. (2006). The influence of magnitude range on empirical ground-motion prediction. *Bulletin of the Seismological Society of America*, 97: 2152 – 2170.

Camelbeeck, T. (1994). *Mécanisme au foyer des tremblements de terre et contraintes*

tectoniques: le cas de la zone intraplaque belge. PhD thesis, Universit Catholique de Louvain and Observatoire Royal de Belgique.

Campbell, K. (1985). Strong motion attenuation relations: a ten year perspective. *Earthquake Spectra*, 1: 759 – 804.

Campbell, K. (1997). Empirical near-source attenuation relationships for horizontal and vertical components of peak ground acceleration, peak ground velocity and pseudo-absolute acceleration response spectra. *Seismological Research Letters*, 68: 154 – 179.

Campbell, K. and Bozorgnia, Y. (2003). Updated near-source ground-motion (attenuation) relations for the horizontal and vertical components of peak ground acceleration and acceleration response spectra. *Bulletin of the Seismological Society of America*, 93 N. 1: 314 – 331.

Campbell, K. and Bozorgnia, Y. (2008). NGA ground motion model for the geometric mean horizontal component of PGA, PGV, PGD and 5ranging from 0.01 to 10 s. *Earthquake Spectra*, 24: 139 – 172.

Cornell, C. (1968). Engineering seismic risk analysis. *Bulletin of the Seismological Society of America*, 58 N. 5: 1583 – 1606.

De Crook, T. (1993). Probabilistic seismic hazard assessment for The Netherlands. *Geologie en Mijnbouw*, 72: 1 – 13.

De Crook, T. (1996). A seismic zoning map conforming to Eurocode 8, and practical earthquake parameter relations for the Netherlands. *Geologie en Mijnbouw*, 75: 11 – 18.

Dost, B., van Eck, T., and Haak, H. (2004). Scaling of peak ground acceleration and peak ground velocity recorded in the Netherlands. *Bollettino di Geofisica Teorica ed Applicata*, 45 N. 3: 153 – 168.

Douglas, J. (2004). An investigation of analysis of variance as a tool for exploring regional differences in strong ground motions. *Journal of Seismology*, 8 N. 4: 485 – 496.

Eck, T. v., Goutbeek, F., Haak, H., and Dost, B. (2006). Seismic hazard due to small-magnitude, shallow-source, induced earthquakes in the Netherlands. *Engineering Geology*, 87: 105 – 121.

Geluk, M., Duin, E., Dusar, M., Rijkers, R., van den Berg, M., and van Rooijen, P. (1994). Stratigraphy and tectonics of the Roer Valley Graben. *Geologie en Mijnbouw*, 73: 129 – 141.

Grünthal, G. (1999). Seismic hazard assessment for Central, North and Northwest Europe: GSHAP Region 3. *Annali di Geofisica*, 42 N. 6: 999 – 1011.

Grünthal, G., Bosse, C., and Stromeyer, D. (2007). Die neue Generation der probabilistischen seismischen Gefährdungseinschätzung der Bundesrepublik Deutschland, Version 2007 mit Anwendung für die Erdbeben-Lastfälle der DIN 19700:2004-07 "Stauanlagen". Scientific technical report STR09/07, Deutsches GeoForschungsZentrum GFZ. 83 p.

Helmholtz Centre Potsdam - GFZ German Research Centre for Geosciences (2008). Seismic Hazard Assessment for the D-A-CH countries (Germany D, Austria A, Switzerland CH). http://www.gfz-potsdam.de/portal/gfz/Struktur/Departments/Department+2/sec26/projects/01_seismic_hazard_assessment/D-A-CH.

Hinzen, K.-G. (2003). Stress field in the Northern Rhine area, Central Europe, from earthquake fault plane solutions. *Tectonophysics*, 377: 325 – 356.

Jimenez, M.-J., Giardini, D., and Grünthal, G. (2003). The ESC-SESAME Unified

Hazard Model for the European-Mediterranean region. *EMSC/CSEM Newsletter*, 19: 2 – 4.

Joyner, W. and Boore, D. (1981). Peak horizontal acceleration and velocity from strong-motion records including records from the 1979 Imperial Valley, California, earthquake. *Bulletin of the Seismological Society of America*, 71: 2011 – 2038.

Leynaud, D., Jongmans, D., Teerlynck, H., and Camelbeeck, T. (2000). Seismic hazard assessment in Belgium. *Geologica Belgica*, 3 (1 – 2): 67 – 86.

Mayer-Rosa, D. and Merz, H. (1976). Seismic risk maps for Switzerland. Description of the probabilistic method and discussion of some input parameters. In Ritsema, A. and Gürpinar, A., editors, *Proc. European Seismological Commission Symposium Luxembourgh*, 153, pages 45 – 52. Royal Netherlands Meteorological Institute.

McGarr, A. (1984). Scaling of Ground Motion Parameters, State of Stress, and Focal Depth. *Journal of Geophysical Research*, 89 N. B8: 6969 – 6979.

McGuire, R. (1976). FORTRAN Computer Program for Seismic Risk Analysis. Open file report 76 – 67, U.S. Geological Survey. 90 p.

Meskouris, K. (2005). Konzepte der DIN 4149. Technical report, RWTH Aachen, Lehrstuhl für Baustatik und Baudynamik. 15 p.

Musson, R. (1999). Determination of design earthquakes in seismic hazard analysis through Monte Carlo simulation. *Journal of Earthquake Engineering*, 3: 463 – 474.

Musson, R. (2009). PSHA using Monte Carlo simulation: M3C v3 User guide. Internal report IR/09/058, British Geological Survey. Personal communications, 31 p.

Musson, R. and Sargeant, S. (2007). Eurocode 8 seismic hazard zoning maps for the UK. Report CR/07/125 issue 3.0, British Geological Survey. 66 p.

Ordaz, M. (1999). CRISIS99. A computer program to compute seismic hazard. Technical report, Authonomous University of Mexico (UNAM).

Reiter, L. (1990). *Earthquake hazard analysis: issues and insights.* Columbia University Press. 254 p.

Risk Engineering, I. (1996). FRISK88M, User's manual. Boulder, Colorado.

Royal Meteorological Institute of the Netherlands (KNMI) (2010a). Lijst met tektonische aardbevingen in de regio rondom Nederland. http://www.knmi.nl/seismologie/tectonische-bevingen-regio.

Royal Meteorological Institute of the Netherlands (KNMI) (2010b). Lijst met tektonische aardbevingen in Nederland. http://www.knmi.nl/seismologie/tectonische-bevingen-nl.

Shakal, A. and Bernreuter, D. (1981). Empirical analyses of near-source ground motion. NUREG/CR-2095, U.S. Nuclear Regulatory Commission.

TERA Corporation (1978). Bayesian seismic hazard analysis, a methodology.

Thenhaus, P. and Campbell, K. (2003). Seismic hazard analysis. In Chen, W.-F. and Scawthorn, C., editors, *Earthquake Engineering Handbook.*, pages 8–1 – 8–50. CRC Press.